

Event-based cooperative control of multi-agent systems for odor source localization in an unknown environment

Thesis by
Abhinav Sinha

In Partial Fulfillment of the Requirements for the
degree of
Master of Technology



INDIAN INSTITUTE OF ENGINEERING SCIENCE AND TECHNOLOGY
Shibpur (Howrah), India

2018
Defended [Exact Date]

© 2018

Abhinav Sinha
ORCID: [0000-0001-6419-2353](https://orcid.org/0000-0001-6419-2353)

All rights reserved

"If I have seen further. . . it is by standing upon the shoulder of giants."

— Sir Isaac Newton

To Yash, mathematician of the 21st century. May your works inspire us all.

To Anamika, who is always a blessing in disguise.

ACKNOWLEDGEMENTS

This thesis is not only representative of my work at the keyboard, but a starting milestone in a full-time career in research ahead. This thesis is also the consequence of numerous experiences I had during my work at Central Scientific Instruments Organization (CSIO), India and many remarkable individuals I met over the duration of two years.

Prima facie, I wish to express my sincere gratitude to my thesis supervisors, Mrs. Rishemjit Kaur (Scientist, CSIO) and Mr. Ritesh Kumar (Scientist, CSIO), who have supported me throughout my thesis with their patience and understanding, while allowing me the room to work things my way. I attribute the level of my master's degree to their encouragement and effort and without them this thesis, too, would not have been completed or written. One simply could not wish for a better or friendlier supervisor.

I also wish to thank Dr. Amol Bhondekar (Principal Scientist, CSIO) for introducing me to robot olfaction, particularly odor source localization, his guidance, and numerous suggestion throughout the work that helped in improving the quality of this thesis.

With honorable mentions, I am also thankful to other staff members of our lab—Dr. Anupma Sharma (Technical Officer, CSIO), Mrs. Monica Singla (Sr. Technical Officer, CSIO), Mr. Saurav Kumar (Scientist, CSIO), Mr. Manu Sharma (Technical Assistant, CSIO), Mr. Shambo Roy Choudhury (Research Scholar, CSIO) and Mr. Varun Saini (Junior Research Fellow, CSIO) for their help and assistance during the work.

I always extend my deepest gratitude towards my family, for believing in me and supporting me in my endeavor. I shall always remain indebted to good teachers, without whom I would not have reached this far. Finally, I am obliged to Mr. Rajiv Kumar Mishra for introducing me to control systems and becoming a companion in my research undertakings. It was only his encouragement that a love for systems and control instigated in me.

CERTIFICATE OF APPROVAL

The research work stated in this thesis has been certified to be done by Mr. Abhinav Sinha under the supervision of Scientists Mrs. Rishemjit Kaur and Mr. Ritesh Kumar, at Central Scientific Instruments Organisation, Chandigarh UT, India.

Mrs. Rishemjit KAUR
Scientist
CSIR– CSIO

Mr. Ritesh KUMAR
Scientist
CSIR– CSIO

Dr. Subhasis BHAUMIK
Coordinator
School of Mechatronics & Robotics
Indian Institute of Engineering
Science and Technology
Shibpur (Howrah), India

Dr. Debjani GANGULY
Head of Department
School of Mechatronics & Robotics
Indian Institute of Engineering
Science and Technology
Shibpur (Howrah), India

DECLARATION

The programme "Mechatronics and Robotics" is offered by Indian Institute of Engineering Science and Technology, Shibpur (Howrah), India in collaboration with three CSIR labs— Central Scientific Instruments Organisation, Central Electronic Engineering Research Institute, and Central Mechanical Engineering Research Institute. The work of Mr. Abhinav Sinha was carried out at Central Scientific Instruments Organisation.

This thesis entitled "Cooperative control of multi-agent systems for odor source localization in an unknown environment" is an original research work carried out by Mr. Abhinav Sinha towards completion of his Master of Technology degree in Mechatronics and Robotics. This work has been composed solely by Mr. Abhinav Sinha, and has not been submitted elsewhere, in whole or in part, in any previous application for a degree. Except where stated otherwise by reference or acknowledgment, the work presented is entirely his own.

ABSTRACT

Inspiration of odor source localization problem stems from behavior of biological entities such as mate seeking by moths, foraging by lobsters, prey tracking by mosquitoes and blue crabs, etc., and is aimed at locating the source of a volatile chemical. These behaviors have long been mimicked by autonomous robot(s). Chemical source tracking has attracted researchers around the globe due to its applications in both civilian and military domains. A plethora of applications are possible, some of which include detection of forest fire, oil spills, release of toxic gases in tunnels and mines, gas leaks in industrial setup, search and rescue of victims and clearing leftover mine after an armed conflict. A plume containing filaments, or odor molecules, is generally referred to the downwind trail formed as a consequence of mixing of contaminant molecules in any kind of movement of air. The dynamical optimization problem of odor source localization can be effectively solved using multiple robots working in cooperation. The obvious advantages of leveraging multi-agent systems (MAS) are increased probability of success, redundancy and improved overall operational efficiency and spatial diversity in having distributed sensing and actuation.

This work is aimed at solving the problem of odor source localization by multi-agent systems operating under communication constraints. A hierarchical cooperative control has been put forward to solve the problem of locating source of an odor by driving the agents in consensus when at least one agent obtains information about location of the source. Synthesis of the proposed controller has been carried out in a hierarchical manner of group decision making, path planning and control. Decision making utilizes information of the agents using conventional Particle Swarm Algorithm and information of the movement of filaments to predict the location of the odor source. The predicted source location in the decision level is then utilized to map a trajectory and pass that information to the control level. The distributed control layer uses event-based sliding mode controllers known for their inherent robustness and the ability to reject matched disturbances completely, as well as providing reduced communication and computational load. Two cases of movement of agents towards the source, i.e., under consensus and formation have been discussed herein. Finally, numerical simulations and performance metrics demonstrate the efficacy of the proposed hierarchical distributed control in both one and two dimensions.

TABLE OF CONTENTS

Acknowledgements	iv
Certificate of Approval	v
Declaration	vi
Abstract	vii
Table of Contents	viii
List of Illustrations	ix
List of Tables	xi
Chapter I: Odor source localization	1
1.1 Introduction	2
1.2 Odor source localization in nature	2
1.3 Significance of odor source localization from engineering viewpoint .	4
Chapter II: Background and preliminaries	6
2.1 Basics of cooperative control	6
2.2 A quick review of spectral graph theory	7
2.3 Fundamentals of sliding mode control	8
2.4 An introduction to event based control	9
Chapter III: Review of the state of the art	12
3.1 Effect of odor dispersal	12
3.2 Towards a mathematical model of odor dispersal	13
3.3 Early works in the odor source localization problem	14
3.4 Existing approaches to the odor source localization problem	15
Chapter IV: Synthesis of the controller	17
4.1 Problem statement	17
4.2 Dynamics of multi-agent systems	18
4.3 Mathematical description of the problem	19
4.4 Distributed hierarchical cooperative control scheme	19
Chapter V: Results of numerical simulation	31
5.1 Source seeking by homogeneous agents	33
5.2 Source seeking by heterogeneous agents	39
Chapter VI: Concluding remarks	46
6.1 Conclusion	46
6.2 Summary of contributions	47
6.3 Outlook towards future research	47
Bibliography	48

LIST OF ILLUSTRATIONS

<i>Number</i>	<i>Page</i>
1.1 Ants locating food source by following pheromone trail (adapted from [1])	3
2.1 An illustration of Riemann and Lebesgue sampling techniques	10
2.2 A simplified block diagram of event-based control in leader-following multi-agent system	11
4.1 Schematic of the proposed hierarchical cooperative control scheme	20
5.1 Interaction topology of agents	31
5.2 Homogeneous agents in consensus to locate source of odor in \mathbb{R}^1	35
5.3 Homogeneous agents in formation to locate source of odor in \mathbb{R}^1	35
5.4 Tracking errors and sliding manifolds in \mathbb{R}^1 during localization via consensus (in context of homogeneous agents)	35
5.5 Sampling intervals of homogeneous agents and the smooth control signal during consensus	36
5.6 Average time consumed by homogeneous agents under time-triggered and event-triggered controls for 50 repeated trials	37
5.7 Norm of tracking errors along both axes in \mathbb{R}^2 (in context of homogeneous agents)	38
5.8 Homogeneous agents in consensus to locate source of odor in \mathbb{R}^2	38
5.9 Homogeneous agents in formation to locate source of odor in \mathbb{R}^2	38
5.10 Heterogeneous agents in consensus to locate source of odor in \mathbb{R}^1	40
5.11 Heterogeneous agents in formation to locate source of odor in \mathbb{R}^1	40
5.12 Tracking errors and sliding manifolds in \mathbb{R}^1 during localization via consensus (in context of heterogeneous agents)	40
5.13 Sampling intervals of heterogeneous agents and the smooth control signal during consensus	41
5.14 Average time consumed by heterogeneous agents under time-triggered and event-triggered controls for 25 repeated trials	42
5.15 Localization by heterogeneous multi-agent systems under the effect of mismatched and matched disturbances	43
5.16 Wind turbulence in the domain during localization via consensus	44
5.17 Wind turbulence in the domain during localization via formation	44

5.18	Norm of tracking errors along both axes in \mathbb{R}^2 (in context of heterogeneous agents)	44
5.19	Heterogeneous agents in consensus to locate source of odour in \mathbb{R}^2	45
5.20	Heterogeneous agents in formation to locate source of odour in \mathbb{R}^2	45

LIST OF TABLES

<i>Number</i>		<i>Page</i>
5.1	Values of the design parameters used in simulation	32
5.2	Four cases of localization by set of homogeneous agents	37
5.3	Performance metrics in context of localization by homogeneous agents	37
5.4	Number of controller updates in the set of homogeneous agents under event-based control law	37
5.5	Four cases of localization via set of heterogeneous agents	42
5.6	Performance metrics in context of localization by heterogeneous agents	43
5.7	Number of controller updates in the set of heterogeneous agents under event-based control law	43

Chapter 1

ODOR SOURCE LOCALIZATION

Of all the ingredients we employ in the creation of a garden, scent is probably the most potent and the least understood. Its effects can be either direct and immediate, drowning our senses in a surge of sugary vapor, or they can be subtle and delayed, slowly wafting into our consciousness, stirring our emotions and coloring our thoughts.

Stephen Lacey

The physiological potencies in living organisms responsible for providing data for perception, are referred as senses. There are many senses according to the aforesaid definition, e.g., vision (sight), audition (hearing), gustation (taste), olfaction (smell), somatosensation (touch), equilibrioception (sense of balance), thermoception (sense of heat), proprioception (kinesthetic sense), nociception (physiological pain), interoception (internal sense such as hunger, etc.), chronoception (perception of passage of time), agency (subjective feeling of having chosen a particular action), familiarity, recollection, echolocation (interpreting reflected sounds), electoreception (interpreting electric field), magnetoreception (interpreting magnetic field based on earth's magnetic field), hygrocception (interpreting moisture content in the environment), etc. Of all these senses, traditionally recognized fundamental senses in humans are vision, audition, gustation, olfaction and somatosensation. In terms of evolution, olfaction is regarded as the oldest sense [2] that allowed the organisms with odorant receptors to identify food, potential mating partners, dangers and enemies. The act of enabling a machine with automated sense of smell is called machine olfaction. When the machine under consideration is a robot, the field of study is generally termed as robot olfaction, of which locating the source of an odor is an integral task.

1.1 Introduction

Odor source localization is generally referred to the task of finding the location of a volatile chemical source in environment. It is a subset of robot olfaction, and has many practical (including humanitarian) applications. An odor plume containing filaments, or odor molecules, is generally referred to the downwind trail formed as a consequence of mixing of contaminant molecules in any kind of movement of air. In odor source localization, the robot traverses through the plume to find a global maximum concentration of the chemical and declares the location to be the location of the source. Thus, this localization problem can be characterized by three stages:

- Search for odor plumes and plume recognition
- Plotting a course towards the source along the plume, guided by the recognition
- Verification and declaration of odor source with certain accuracy

Odor source localization using robots is an emulation to the use of sniffing animals such as dogs, etc. In case of robot(s), the three stages in localization can be described as instantaneous plume sensing, robot maneuvering, and control of the robot. In general, there exists two approaches to solve this problem— forward approach and inverse approach. In the former, the state of the odor is estimated in advance, whereas in the latter one, the current state of the odor is used to estimate the previous state of the odor. In either approach, the localizing algorithms are required that enable the robot(s) to make a transition from the present location to the predicted location (location of the source). There are several biological entities in nature which use odor source localization in their day-to-day activities. Hence, biological odor localization is the prime source of inspiration behind robot olfaction.

1.2 Odor source localization in nature

At this point we introduce the term chemotaxis and anemotaxis, which shall be used quite often in the coming text. *Chemotaxis* has been defined by *Merriam–Webster Medical Dictionary* as “orientation or movement of an organism or cell in relation to chemical agents.” In a similar fashion, according to *Random House Unabridged Dictionary*, “oriented movement in response to a current of fluid” is referred as *anemotaxis*.

There are several instances in nature where chemotactic behavior of biological entities leads to odor source localization. By virtue of this phenomenon, moths

seek mating partners, lobsters locate food source, mosquitoes and blue crabs track their prey, and parasitoid wasps locate hosts. There are several organisms like fish which use this property predominantly to locate food. Microorganisms, bacteria (e.g. *Escherichia coli*), etc. are also known to use odor source localization to locate nutrients. Ants use pheromone trails to locate food. The following illustration has been presented to describe how ants are able to find food source.

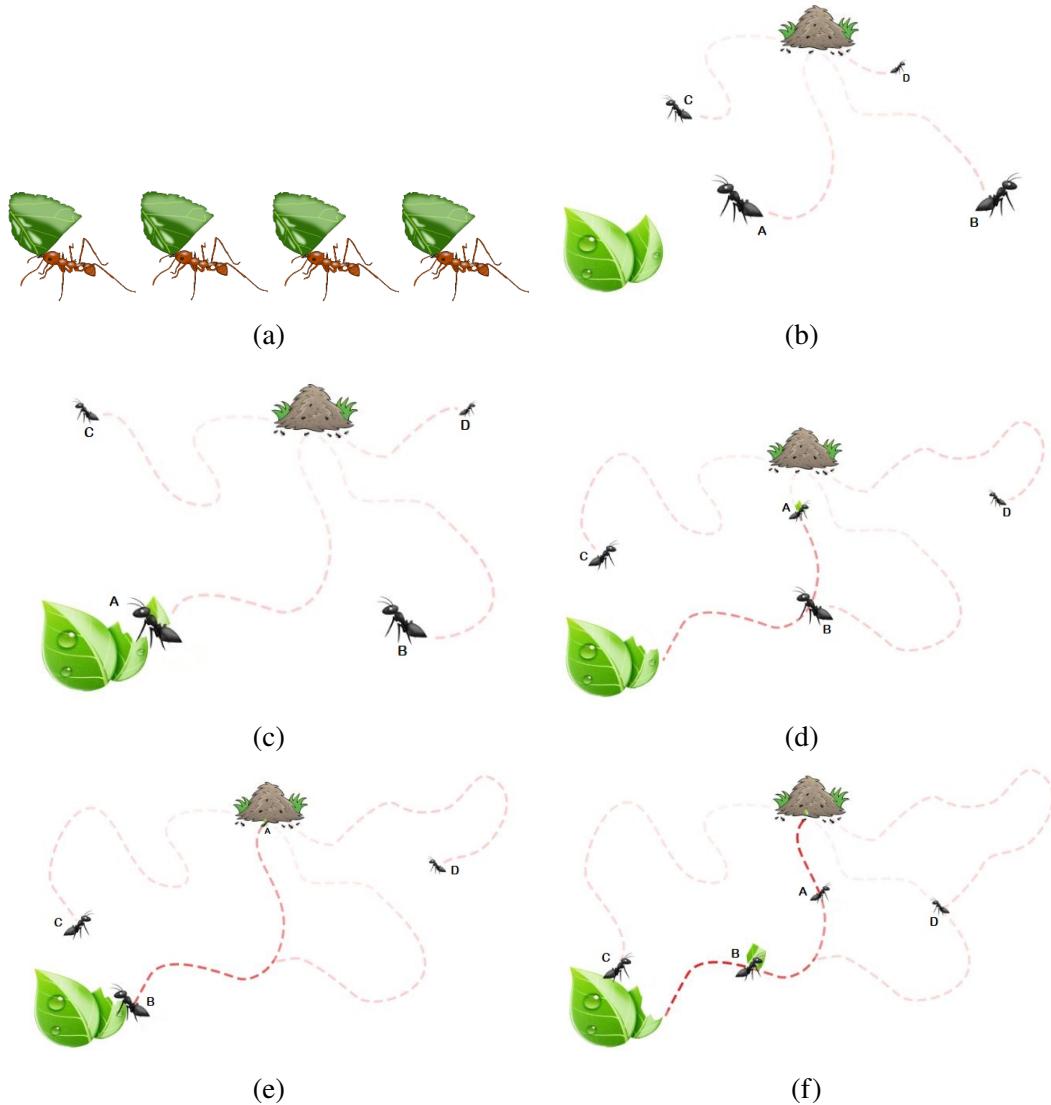


Figure 1.1: Ants locating food source by following pheromone trail (adapted from [1])

Ants form a single queue after finding food (fig. 1.1a). The complete process of locating food is dependent on finding pheromone trails of neighboring ants. Suppose there are four neighboring ants named A, B, C and D, a food source and an ant hill.

Each ant is located at random position and deposits some traces of pheromones along its search path. When none of the ants is carrying food, each ant tends to pick up the strongest pheromone trail that it can find. When food source, or the pheromone trail is absent, ants explore the region for food in a random fashion (fig. 1.1b). Pheromones deposited by ants do not last long and start to decay. Hence, ants pick up the strongest trail they can find and march along the shortest route to save time. Now, let us assume that the ant A finds food source and carries some food to the ant hill (fig. 1.1c). Ant A follows its own pheromone back to the hill, and along its way, it deposits more pheromones to make the trail stronger. During random exploration, ant B finds ant A's pheromones (fig. 1.1d). Using ant A's reinforced pheromone trail, ant B also locates the food source (fig. 1.1e), picks some food, and marches towards the hill to deposit its contribution. During its way back home, ant B also deposits pheromones to further make the trail stronger. There are two ways for ant B to go back home— its own trail and the trail of ant A. Since the trail of ant A is stronger, ant B tends to traverse along ant A's trail (fig. 1.1f). In the meantime, ant C also finds the food using its own trail. However, ant C abandons its own trail for a stronger trail laid out by ants A and B (fig. 1.1f).

1.3 Significance of odor source localization from engineering viewpoint

Robot olfaction has grown to become a prominent research area owing to numerous advantages offered by mobile agents that can emulate sensing capabilities. From the standpoint of engineering, we envisage many applications in which sniffing robots find significance. First and foremost, robots can be deployed in places where humans (or dogs for that matter) can't. This enables a sniffing robot to be executed in locating forest fire, gas leaks, oil spills, detection of hazardous substances, unexploded mines after an armed conflict, etc. In indoor and industrial setups, an electronic nose can be installed to sample the air in a continuous manner and to act in a closed-loop fashion. Moreover, odor source localization can also be used to detect drugs in customs and quarantine applications, search and rescue of victims in an earthquake damaged building, landslides or avalanches. Sometimes, odor localization can be used to locate other agents in multi-agent systems. Olfaction can also be used to complement other sensing capabilities such as vision.

For instance, when we perceive the smell of food being cooked, we reason that somebody must be in kitchen. This means that our perception of smell has been associated with some human activity in this case. Similarly, when we smell butane, we rush to the kitchen instead of going elsewhere. In the kitchen, we immediately

check those appliances using a butane/gas connection. Therefore, there is a complex and an intelligent mechanism of perception of odor in the environment that utilizes sensor data fusion, closed loop activity and semantic information.

Recently, odor source localization using autonomous agents has also been carried out on Mars [3–7]. The extent of application of this particular task is huge. A successful odor localization requires synergistic integration of many engineering disciplines such as electronics engineering, mechatronics, control engineering, mechanical engineering, computer science engineering, communication engineering and information technologies.

Chapter 2

BACKGROUND AND PRELIMINARIES

The object of our lives is to look
 at, listen to, touch, taste things.
 Without them, – these sticks,
 stones, feathers, shells, – there is
 no Deity.

R. H. Blyth

While research on robot olfaction is inherently complex and has been addressed from a wide perspective, we have carried out odor localization using multiple mobile agents working in cooperation. As established earlier, there are three stages in robot olfaction— instantaneous plume sensing, robot maneuvering, and control of the robot. Our study is concentrated on the control of robots in a multi-agent swarm tasked to locate source of an odor as a collective entity. Keeping in view to enhance the reading comprehension of the coming text and computations, a threshold of discussion on essential topics has been provided in this chapter.

2.1 Basics of cooperative control

Complex systems such as social systems, biological systems, science and engineering systems often consist of heterogeneous entities having individual characteristics. They interact with each other in several ways, and exhibit certain group phenomena. The intriguing animal group behaviors and observations in nature such as the groups of ants, schools of fish, flock of birds, swarm of bacteria, etc. have led to the development of protocols for cooperative control. Owing to the sophisticated interactions existing among the agents, these systems are often modeled as networked systems. Their characteristics and behaviors are manifestations of the protocols governing each agent's role and impact in the multi-agent systems.

In a networked system, such as multi-agent systems or large scale interconnected systems, there are many sub-systems. A cooperative control requires that the state trajectories of each sub-system move in a collaborative manner to achieve a common goal. This common goal, or objective is characterized by equilibrium point(s).

Unlike a standard stability problem, these equilibrium point(s) may not be known in priori, rather have to be decided in real time, e.g., in odor source localization. This is due to several factors such as different initial conditions, change in system dynamics and effect of the environment.

When a number of sub-systems are networked, there are several sensors or communication links or a combination of both. Agents in multi-agent systems use these to exchange information among themselves and also to interact with the environment. Associated with communication links are latency, noise, packet loss, limited bandwidth, etc., thereby requiring cooperative controllability. Even a small perturbation in a single agent can adversely affect the whole network. Hence, a high degree of autonomy is required with a number of sub-systems getting networked.

Mathematically, a system $\dot{z} = g(z, t, u)$ is said to be cooperatively stable, if for every given $\Theta > 0$, \exists a constant $\vartheta(t_0, \Theta) > 0$ for initial condition $z(t_0)$ that satisfies $\|z_i(t_0) - z_j(t_0)\| \leq \vartheta$ and $\|z_i(t) - z_j(t)\| \leq \Theta, \forall i, j \in \mathbb{N}, i \neq j$ and $t \geq t_0$. The system is said to be asymptotically cooperatively stable if it is cooperatively stable and if $\lim_{t \rightarrow \infty} = c_0 \mathbf{1}$, where $c_0 \in \mathbb{R}$ depends on the initial condition $z(t_0)$ and changes in the dynamics. The system is called uniformly asymptotically cooperatively stable if it is asymptotically cooperatively stable, if $\vartheta(t_0, \Theta) > 0 = \vartheta(\Theta)$ and if the convergence of $\lim_{t \rightarrow \infty} = c_0 \mathbf{1}$ is uniform.

2.2 A quick review of spectral graph theory

A directed graph, also known as digraph [8] is represented here by $\mathcal{G} = (\mathcal{V}, \mathcal{E}, \mathcal{A})$. \mathcal{V} is the nonempty set that contains finite number of vertices or nodes [9, 10] such that $\mathcal{V} = \{1, 2, \dots, N\}$. \mathcal{E} denote edges that are directed and are represented as $\mathcal{E} = \{(i, j) \forall i, j \in \mathcal{V} \& i \neq j\}$. \mathcal{A} is the weighted adjacency matrix such that $\mathcal{A} = a(i, j) \in \mathbb{R}^{N \times N}$.

The existence of an edge (i, j) is only possible if and only if the vertex i receives the information supplied by the vertex j , i.e., $(i, j) \in \mathcal{E}$. Hence, i and j are referred to as neighbors. Let us consider a set \mathcal{N}_i that contains labels of vertices that are neighbor of the vertex i . For the adjacency matrix \mathcal{A} , $a(i, j) \in \mathbb{R}^+ \cup \{0\}$. If $(i, j) \in \mathcal{E} \Rightarrow a(i, j) > 0$. If $(i, j) \notin \mathcal{E}$ or $i = j \Rightarrow a(i, j) = 0$.

The Laplacian matrix \mathcal{L} [8, 11, 12] lies at the heart of the consensus problem and is given by $\mathcal{L} = \mathcal{D} - \mathcal{A}$ where \mathcal{D} is a diagonal matrix, i.e, $\mathcal{D} = \text{diag}(d_1, d_2, \dots, d_n)$ whose entries are $d_i = \sum_{j=1}^n a(i, j)$. \mathcal{D} is known as degree matrix in the notions of graph theory. A directed path from vertex j to vertex i defines a sequence comprising

of edges $(i, i_1), (i_1, i_2), \dots, (i_l, j)$ with distinct vertices $i_k \in \mathcal{V}$, $k = 1, 2, 3, \dots, l$. \mathcal{B} is also a diagonal matrix with entries 1 or 0 and is commonly referred as incidence matrix. If there exists an edge between leader agent and any other agent, the entry is 1, otherwise the entry is 0. Furthermore, it can be inferred that the path between two distinct vertices is not uniquely determined. However, if a distinct node in \mathcal{V} contains directed path to every other distinct node in \mathcal{V} , then the directed graph \mathcal{G} is said to have a spanning tree.

Physically, each agent in multi-agent systems is represented by a vertex or a node and the line of communication between any two agents is represented as a directed edge. The relationship between \mathcal{G} and \mathcal{V} establishes the following lemmas.

Lemma 2.2.1. *Consider a directed graph \mathcal{G} and its Laplacian matrix \mathcal{L} . The set of eigenvalues of \mathcal{L} contains at least one zero eigenvalue. Other nonzero eigenvalues of \mathcal{L} have positive real parts. \mathcal{L} has a simple zero eigenvalue only when \mathcal{G} has a spanning tree. Also, \mathcal{G} is said to be balanced if the following criterion is met:*

$$\mathcal{L}\mathbf{1}_N = \mathbf{1}_N^T \mathcal{L} = \mathbf{0}_N. \quad (2.1)$$

Here $\mathbf{1}_N$ denotes a column vector of all 1s, i.e., $[1, 1, \dots, 1]^T$ and $\mathbf{0}_N$ denotes a column vector of all 0s, i.e., $[0, 0, \dots, 0]^T$. Both $\mathbf{1}_N$ and $\mathbf{0}_N \in \mathbb{R}^N$. The elements of \mathcal{L} are denoted as $l(i, j)$ such that $l(i, j) \in \mathbb{R}^{N \times N}$.

Lemma 2.2.2. *The matrix $\mathcal{L} + \mathcal{B}$ has full rank when \mathcal{G} has a spanning tree with leader as the root. This implies non singularity of $\mathcal{L} + \mathcal{B}$.*

Proofs of the lemmas described above can be found in [11] and thus, are omitted here.

2.3 Fundamentals of sliding mode control

Pioneering works on sliding mode control originated in former Soviet Union in early 1960s. Sliding Mode Control (SMC) [13–16] is a particular type of variable structure control that is known for its inherent robustness. The switching nature of the control is used to nullify bounded disturbances and matched uncertainties. Switching happens about a hypergeometric manifold in state space known as sliding manifold, surface, or hyperplane. The control drives the system monotonically towards the sliding surface, i.e, trajectories emanate and move towards the hyperplane (reaching phase). System trajectories, after reaching the hyperplane, get constrained there

for all future time (sliding phase), thereby ensuring the system dynamics remains independent of bounded disturbances and matched uncertainties.

In order to push state trajectories onto the surface $s(x)$, a proper discontinuous control effort $u_{\text{SM}}(t, x)$ needs to be synthesized satisfying the following inequality.

$$s^T(x)\dot{s}(x) \leq -\eta\|s(x)\|, \quad (2.2)$$

with η being positive and is referred as the reachability constant.

$$\therefore \dot{s}(x) = \frac{\partial s}{\partial x} \dot{x} = \frac{\partial s}{\partial x} f(t, x, u_{\text{SM}}) \quad (2.3)$$

$$\therefore s^T(x) \frac{\partial s}{\partial x} f(t, x, u_{\text{SM}}) \leq -\eta\|s(x)\|. \quad (2.4)$$

The motion of state trajectories confined on the manifold is known as *sliding*. Sliding mode exists if the state velocity vectors are directed towards the manifold [13, 17] in its neighborhood. Under such consideration, the manifold is called attractive, i.e., trajectories starting on it remain there for all future time and trajectories starting outside it tend to it in an asymptotic manner. Hence, in sliding motion,

$$\dot{s}(x) = \frac{\partial s}{\partial x} f(t, x, u_{\text{SM}}) = 0. \quad (2.5)$$

$u_{\text{SM}} = u_{eq}$ is a solution, generally referred as equivalent control is not the actual control applied to the system but can be thought of as a control that must be applied on an average to maintain sliding motion and is mainly used for analysis of sliding motion.

2.4 An introduction to event based control

With the advancement of embedded systems, almost all the controllers are realized in sampled data approach owing to its easy implementation properties. Therefore, the practical approach to solve leader follower consensus problem is to use sampled data control especially in bandwidth and energy constrained environments. The traditional sampled data control system considers periodic update of the controllers even after achieving control objective. The measurements are sampled and control is updated periodically even if the system may tolerate fluctuations in some allowable range. This results in wastage of significant computational and communication resources. An efficient way to reduce communication and computational burden is to use event triggering scheme. The samples are obtained only when an event is triggered. The objective of the event triggering scheme is to sample and update

controller only when the local measurement error crosses a predefined threshold while ensuring satisfactory closed loop performance of the system.

In practice, individual autonomous agents in multi-agent systems are often equipped with small digital microcontrollers to reduce the cost. These microcontrollers have limited computing and communication capabilities. According to traditional sampled data control systems theory, samples of a measured output are obtained in periodic fashion with a fixed sampling rate. In addition to this a zero order hold operator is needed to maintain the control input signal constant between successive sample instants. This sampling technique is known as periodic sampling and is generally done along the time axis, also known as *Riemann* sampling [18] (figure 2.1a). An alternative and more efficient way to obtain samples along dependent variable axis (vertical axis), known as *Lebesgue* sampling [18] (2.1b). Under this

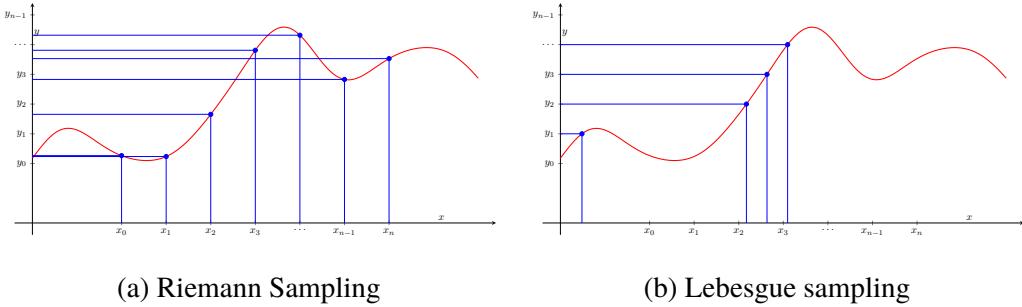


Figure 2.1: An illustration of Riemann and Lebesgue sampling techniques

technique, sampling interval is no longer periodic and samples are obtained only when a *noticeable change*, also referred to as an *event* occurs. As a result, the controller does not need to update itself periodically, but a hold type operator is still needed to maintain the value constant between successive sample instants. The continuous sampling and transmission, along with the occupancy of central processing unit to perform computations when the signal is constant (not changing too frequently) leads to significant wastage of available resources. The optimum utilization of communication, computing and energy expenses is a concern in various applications with increasing number of systems getting networked. One mitigation strategy adopted is event based control wherein control is applied only when the system calls for it depending upon some *event*. Event-based sampling is a trade-off between performance and sampling frequency. Interested reader can refer [19–30].

As a consequence of combining event-based strategies with sliding mode control, the robustness of the system has been retained while maintaining lower computational

expense. However, the system trajectories tend to move away from the sliding manifold till the control is updated again but remain bounded within a band.

A simplified block diagram of event-based control in leader-following consensus of multi-agent systems has been illustrated in figure 2.2. The dotted lines represent discrete signals, i.e., at $t = t^k$ instants, and the solid lines represent continuous signals. The overall system is hybrid. $x(t)$, $v(t)$ and $u(t)$ are position states, velocity states and control signal associated with the agents respectively.

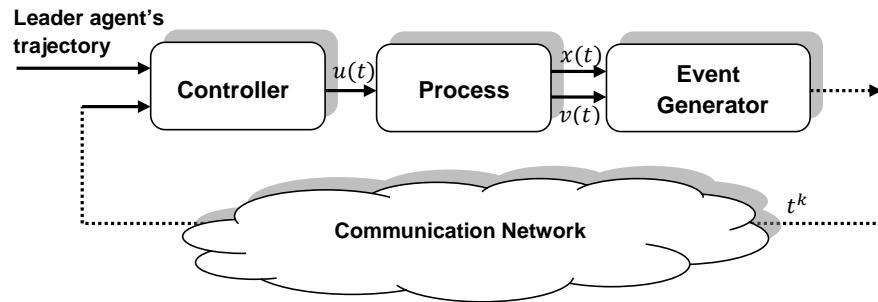


Figure 2.2: A simplified block diagram of event-based control in leader-following multi-agent system

Chapter 3

REVIEW OF THE STATE OF THE ART

Nothing revives the past so completely as a smell that was once associated with it.

Vladimir Nabokov

In terms of olfactory potencies, several animals such as dogs, rodents and fish surpass humans. It is due to this advantage that even to this date, animals such as dogs are still used in many applications. Successfully emulating the behavior of organisms for odor localization led to the development of static electronic noses [31], that were placed in various setups to measure odor concentrations at multiple locations and declare the location with maximum concentration. The problem with static electronic noses are they can't detect odor concentrations that do not reach their reactive sensory surface. To mitigate this hurdle in solving odor source localization problems, electronic noses and or various gas sensors needed to be mounted on a mobile platform, preferably a mobile robot to cover wider area and varying odor concentration patches. This led to the development of mobile robot olfaction. In this chapter, we shall consider the effect of odor dispersal, and a brief review on several odor source localization techniques using robot(s).

3.1 Effect of odor dispersal

Despite several developments in sensing technologies, the absence of faster odor localizing algorithms and intelligent control techniques are still a challenge. The extent to which a localizing technique is suited to the environmental conditions determines the success rate in robot olfaction. For this reason, it is necessary to consider the dispersion of odor molecules, or odor filaments in environment. The Reynold's number of the flow is paramount in determining the way in which the odor is dispersed. Viscosity predominates in low values of Reynold's number [32], and there are smooth variations in chemical concentrations. As the Reynold's number increases to high values, odor dispersal is characterized by turbulence. This leads to meandering of the odor plume and the plume becomes patchy. An odor plume is formed when the odor filaments released from the source get carried away by

wind. As odor molecules move away from source, the concentration decreases at the source. Under such scenario, shape of the odor plume is determined by molecular diffusion and turbulent diffusion phenomena. Molecular diffusion imparts random motion to the molecules, gradually moving them apart. Turbulent diffusion has a tendency to tear apart the cloud of molecules with high turbulence of air. The effect of molecular diffusion can be neglected while considering the shape of the plume, but there is no definitive shape of odor plume under turbulent diffusion. Thus, lack of a definitive plume model obstructs the success rate of localizing algorithms. Which dispersion phenomenon/model should be chosen is then just a matter of choice and the context of application.

Odor measurements are also affected by other environmental variables such as temperature, humidity, etc. These factors also contribute to the unpredictable nature of odor dispersal. Moreover, ephemeral nature of odor plume makes it difficult to gas map any environment. At two given segments of time, there is a fine possibility of very huge difference between olfactory environment settings. Most of metal oxide gas sensors available in market exhibit good sensitivity but larger response time [33] (sometimes greater than 10 seconds). This means that they have to be exposed for a long time to get a steady concentration value before sampling next measure. In practice, the nature and shape of the plume have a high tendency to change in such a long duration.

3.2 Towards a mathematical model of odor dispersal

If a prior knowledge of behavior of odor molecules be known, the efficiency and success rates of odor localizing algorithms can be improved drastically. Several researchers have tried to model the behavior of plume based on odor concentration and distribution. A known mathematical model can aid in localizing as well as analyzing rapid changes in olfactory environment. It would not be false to state alternately that a mathematical model can certainly obviate the shortcomings of relying on odor dispersion to a great extent.

A vast majority of works used Gaussian plume model introduced in [34], wherein it was assumed that there exists a point odor source with a three dimensional concentration field. It was also assumed that the meteorological condition and plume emission were stationary. A mathematical model based on movement of odor filaments (odor molecules) was proposed by Farell [35] in which three simulated plume data were analyzed— long term time average, amplitude statistics and temporal statis-

tics. This model [35] was also based on dispersion model of Gaussian distribution that facilitates computational requirements and eases in numerical simulations. By virtue of this nature, we shall use a very close variant of this model in our research. A pseudo-Gaussian plume model based on probability density function of mean odor concentration in three dimensions was proposed in [36], but is less widely used compared to that in [35].

3.3 Early works in the odor source localization problem

Research in mobile robot olfaction started with the deployment of a single mobile agent in the field. Some of the early works reported on odor source localization date back to 1984 when Larcombe *et al.* [37] discussed application of chemically sensitive robots in nuclear industry by considering a chemical gradient based odor dispersal. During 1990s, a lot of work incorporating chemical gradient based approaches have been reported. See [38–40] and references therein, in which the odor dispersal was assumed smooth and diffusion dominated. However, in practice, this assumption leads to poor performance for above-ground agents owing to the geometry and dimensions of the agents used. For underground search, this assumption might be valid and satisfactory results have been obtained, as illustrated in [41–43]. In order to overcome difficulties associated with diffusion dominated odor dispersal model, reactive plume tracking was put forward whose performance was improved by combining vision with sensing [44–46].

An odor compass using wind direction and concentration gradient as useful information has also been used in several researches [47–49] to determine the direction of the odor source. The rate of diffusion of odor filaments is comparatively slower than the wind velocity, causing the odor filaments to be swept downwind. Due to this, the concentration gradient along the wind decreases rendering instantaneous gradient dependency incommodious. There lies a huge unpredictability in locating the true source using such methods. An olfactory assisted mask [50] uses similar principle, and hence can't be used in rapidly changing environments. Algorithms such as chemotaxis [51], anemotaxis [52, 53], infotaxis [54] and fluxotaxis [55, 56] heavily relied on sensing capabilities of the agent. Agent maneuvering techniques were also based on bio-inspired algorithms some of which include Braitenberg style [57], E. coli algorithm [58], Zigzag dung beetle approach [59], silkworm moth style [41, 60, 61] and their variants. However, the efficiency of such algorithms was limited by the quality of sensors, and the manner in which they were used. Most of these techniques also failed to consider turbulence dominated flow and resulted in

poor tracking performance.

The dynamical optimization problem of odor source localization can be effectively solved using multiple agents working in cooperation. The obvious advantages of leveraging multi-agent systems (MAS) are increased probability of success, redundancy, improved overall operational efficiency and spatial diversity in having distributed sensing and actuation. A tremendous growth of research attention towards cooperative control has been witnessed in the past decade [62–65] but very few have addressed the problem of locating source of an odor.

3.4 Existing approaches to the odor source localization problem

Hayes *et al.* [66] proposed a distributed cooperative algorithm based on swarm intelligence for odor source localization and experimental results proved multiple robots perform more efficiently than a single autonomous robot. A Particle Swarm Optimization (PSO) algorithm [67] was proposed by Marques *et al.* [68, 69] to tackle odor source localization problems. To avoid trapping into local maximum concentrations, modified PSO algorithms based on electrical charge theory, where neutral and charged robots have been used, have been proposed [69]. Lu *et al.* [70] proposed a distributed coordination control protocol based on PSO to address the problem. PSO introduces exploratory behavior in the swarm, which aids in locating the source. However, it should be noted that simplified PSO controllers are a type of proportional-only controller and the operating region gets limited between the global and the local best. This needs complicated obstacle avoidance algorithms and results in high energy expenditure. Lu *et al.* [71] also proposed a cooperative control scheme to coordinate multiple robots to locate odor source in which a particle filter has been used to estimate the location of odor source based on wind information, a movement trajectory has been planned, and finally a cooperative control scheme has been used to coordinate movement of robots towards the source.

It is worthy to note that the dynamical models used in these works are oversimplified to integrator dynamics, and the account of unknown perturbations seems to be overlooked. Moreover, the control algorithms that have been used prove ineffective in stabilizing non-holonomic systems, such as differentially driven mobile robots. In practice, it is always necessary to converge the multi-agent systems towards the odor source as quickly as possible. Moreover, most of the studies so far have considered a homogeneous set of agents. Truly homogeneous agents are very hard to obtain as it has been observed that even a set of truly homogeneous agents inevitably drift

towards heterogeneity over time and continued operation. Further, almost every scheme proposed in the context has assumed no restriction on communication and computational capabilities. Investigating the cooperative control of MAS for OSL under bandwidth and energy constrained environments is still a challenge. The influence of limited communication in PSO search strategy has been studied in [72] wherein a probability PSO algorithm has been designed using an information sharing matrix.

A successful odor source localization is an amalgam of quantitative analysis of chemical odor and trajectory mapping algorithms under mercurial environment. Apart from the methods of localization mentioned above, some of the algorithms that find use in odor localization are triangulation algorithm, least squares method, and maximum likelihood estimation.

Chapter 4

SYNTHESIS OF THE CONTROLLER

Sweat is the cologne of
accomplishment.

Heywood Hale Broun

Motivated by the aforementioned studies and to mitigate the challenges associated with this localizing task, we have implemented a robust and powerful hierarchical cooperative control strategy to tackle the problem. The purpose of this study is to devise intelligent control protocols and minimize uncertainty and perturbations in large-scale interconnected multi-agent systems tasked to locate source of an odor. It has been shown in this study that using the proposed control framework, the odor source localization task can be completed with a success rate of 100% and in lesser time compared to studies in [68, 73], implying a faster convergence towards the source of odor. Moreover, we have also accounted for the fact that a time varying disturbance is unavoidable under such operation. Hence, the localization has been carried out in the presence of exogenous perturbations. The overall control scheme has been described in upcoming discussions.

4.1 Problem statement

Leveraging multi-agent systems adds to the overall economy of the challenge. There are multiple agents that individually add to the cost, as well as there is a cost to maintain the communication link and telemetry when these agents are out in the field. However, the advantages offered by such an arrangement clearly surpass those using a single robot. A multi-agent system can search a larger region, and often the localization is faster than a single agent. In this study, we aim to synthesize a robust controller that is intelligent enough to enable the multi-agent systems to accomplish the odor source localization task under communication constraints. We shall carry out synthesis of the controller in such a way that the same discussion applies to localization in n -dimensions.

4.2 Dynamics of multi-agent systems

Consider first order heterogeneous multi-agent systems with a virtual leader and a finite number of followers interacting among themselves and their environment in a well defined directed topology. Under such interconnection, only local information about the predicted location of source of the odor through instantaneous plume sensing is available via communication among agents. The governing dynamics of first order heterogeneous multi-agent systems that comprise of N agents can be written mathematically as

$$\dot{x}_i(t) = f_i(x_i(t)) + u_{SM_i}(t) + \varsigma_i; \quad i \in [1, N] \in \mathbb{N}, \quad (4.1)$$

where $f_i(\cdot)$ denotes the uncertain dynamics of each agent. x_i and u_{SM_i} are the state of i^{th} agent and the associated control respectively. ς_i represents bounded exogenous disturbances that enter the system from input channel, i.e., $\|\varsigma_i\| \leq \varsigma_{max} < \infty$.

Assumption 4.2.1. $f_i(\cdot) : \mathbb{R}^+ \times X \rightarrow \mathbb{R}^m$ is locally Lipschitz over some domain $\mathbb{D}_{\mathbb{L}}$ with Lipschitz constant \bar{L} . For our case, we shall take this domain $\mathbb{D}_{\mathbb{L}}$ to be fairly large. $X \subset \mathbb{R}^m$ is a domain in which origin is contained.

Since the function $f_i(\cdot)$ is uncertain, a nominal system model can be extracted from the known part of the uncertain function $f_i(\cdot)$, and the unknown part can be treated by worst case bounds. The dynamics of each agent is affected by the interconnection among agents as well as the presence of inherent non-linearity in each agent. Note that when $f_i(\cdot) = 0$, the dynamics reduce to those of integrator systems. When $f_i(\cdot) = f(\cdot)$, the dynamics reduce to those of homogeneous agents.

Assumption 4.2.2. We assume that the function $f_i(\cdot)$ is input-to-state stable (ISS) in the sense of Sontag [74]. Recall that a system $\dot{z} = g(z, t, u)$ is said to be ISS if there exist functions $\beta \in \mathcal{KL}$ and $\gamma \in \mathcal{K}$ such that for any initial condition $z(t_0)$ and any bounded input $u(t)$, the solution $z(t)$ exists for all time $t \geq t_0$ and the following criterion is satisfied:

$$\|z(t)\| \leq \beta(z(t_0), t) + \gamma(\|u(t)\|_\infty). \quad (4.2)$$

It is also worthy to note that whenever a feedback law stabilizes the system, there also exists a (possibly different) feedback such that the system with external input is ISS. [74].

Remark 1. For brevity, we shall carry out the discussion in \mathbb{R}^1 . However, the same can be extended to higher dimensions by the use of Kronecker products.

4.3 Mathematical description of the problem

The problem of odor source localization can be viewed as a cooperative control problem in which control laws $u_{SM_i}(t)$ need to be designed such that the conditions $\lim_{t \rightarrow \infty} \|x_i(t) - x_j(t)\| = 0$ and $\lim_{t \rightarrow \infty} \|x_i(t) - x_s(t)\| \leq \theta$ are satisfied. Here $x_s(t)$ represents the probable location of odor source & θ is an accuracy adjustment parameter in declaration of the true location of the source.

4.4 Distributed hierarchical cooperative control scheme

Synthesis of a robust controller operating under communication constraints is the motivation of this study. Event-based control scheduling has become popular in such constrained settings. As opposed to uniformly sampled periodic update of the control signal, in this scheme the controller is updated with a new value only when the measurement error crossed a designer fixed accuracy threshold. Owing to non-trivial odor propagation, and dynamic and turbulent nature of odor plumes, wide fluctuations are observed in measured concentrations. The downwind movement of odor molecules provides effective information on the relative position of the source and hence we have utilized concentration information as well as wind information to predict a probable location of the source. This probable location is then fed to the tracking controller designed on the paradigms of event-based sliding modes. The information about the source via instantaneous sensing and swarm intelligence is obtained in the first layer. Second layer is designed to maneuver the agents via traditional surging, casting and searching methods, i.e., trajectory of the leader agent is mapped in this layer. Third layer is based on event-triggered sliding mode control, where the information obtained in the first layer is passed as a reference to the tracking controller.

Group decision making

This layer utilizes both concentration and wind information to predict the location of odor source. Then, the final probable position of the source can be described as

$$\phi(t_h) = k_1 p_i(t_h) + (1 - k_1) q_i(t_h). \quad (4.3)$$

With the knowledge of PSO, $p_i(t_h)$ in (4.3) can be described as the oscillation center. Information of the wind is captured in $q_i(t_h)$. $k_1 \in (0, 1)$ denotes additional weighting coefficient.

Remark 2. Since the sensors equipped with the agents can only receive data at discrete instants, the arguments in (4.3) represent data captured at $t = t_h$ instants

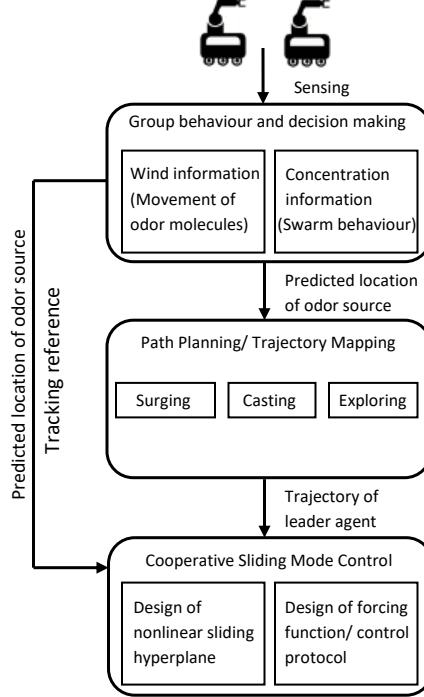


Figure 4.1: Schematic of the proposed hierarchical cooperative control scheme

$(h = 1, 2, \dots)$.

It should be noted that ϕ is the tracking reference that is fed to the tracking controller. Now, we present detailed description of obtaining $p_i(t_h)$ and $q_i(t_h)$.

Commonly used simple PSO algorithm can be described in following form.

$$v_i(t_{h+1}) = \omega v_i(t_h) + u_{\text{PSO}}(t_h), \quad (4.4)$$

$$x_i(t_{h+1}) = x_i(t_h) + v_i(t_{h+1}). \quad (4.5)$$

Here ω is the inertia factor, $v_i(t_h)$ and $x_i(t_h)$ represent the respective velocity and position of i^{th} agent. This commonly used form of PSO can also be used as a proportional-only type controller, however for the disadvantages highlighted earlier, we do not regard PSO as our final controller. PSO control law u_{PSO} can be described as

$$u_{\text{PSO}} = \alpha_1(x_l(t_h) - x_i(t_h)) + \alpha_2(x_g(t_h) - x_i(t_h)). \quad (4.6)$$

In (4.6), $x_l(t_h)$ denotes the previous best position and $x_g(t_h)$ denotes the global best position of neighbors of i^{th} agent at time $t = t_h$, and α_1 & α_2 are acceleration coefficients. Since, every agent in multi-agent systems can get some information about the magnitude of concentration via local communication, position of the agent

with a global best can be easily known. By the idea of PSO, we can compute the oscillation center $p_i(t_h)$ as

$$p_i(t_h) = \frac{\alpha_1 x_l(t_h) + \alpha_2 x_g(t_h)}{\alpha_1 + \alpha_2}, \quad (4.7)$$

where

$$x_l(t_h) = \arg \max_{0 < t < t_{h-1}} \{g(x_l(t_{h-1})), g(x_l(t_h))\}, \quad (4.8)$$

$$x_g(t_h) = \arg \max_{0 < t < t_{h-1}} \{g(x_g(t_{h-1})), \max_{j \in N} a_{ij} g(x_j(t_h))\}. \quad (4.9)$$

Thus, from (4.6), (4.7)

$$u_{\text{PSO}}(t_h) = (\alpha_1 + \alpha_2)\{p_i(t_h) - x_i(t_h)\}, \quad (4.10)$$

which is clearly a proportional-only controller with proportional gain $\alpha_1 + \alpha_2$, as highlighted earlier.

In order to compute $q_i(t_h)$, movement process of a single filament that consists several odor molecules has been modeled based on study in [35]. If $x_f(t)$ denotes position of the filament at time t , $\bar{v}_a(t)$ represent mean airflow velocity and $n(t)$ be some random process, then the model can be described as

$$\dot{x}_f(t) = \bar{v}_a(t) + n(t). \quad (4.11)$$

Without loss of generality, we shall regard the start time of our experiment as $t = 0$.

From (4.11), we have

$$x_f(t) = \int_0^t \bar{v}_a(\tau) d\tau + \int_0^t n(\tau) d\tau + x_s(0). \quad (4.12)$$

$x_s(0)$ denotes the real position of the odor source at $t = 0$.

Assumption 4.4.1. *We assume the presence of a single, stationary odor source. Thus, $x_s(t) = x_s(0)$.*

Implications from remark 2 require (4.12) to be implemented at $t = t_h$ instants. Hence,

$$x_f(t_h) = \sum_{m=0}^t \bar{v}_a(\tau_m) \Delta t + \sum_{m=0}^t n(\tau_m) \Delta t + x_s(t_h), \quad (4.13)$$

$$x_f(t_h) = x_s(t_h) + \bar{v}_a^\star(t_h) + w^\star(t_h). \quad (4.14)$$

In (4.14), $\sum_{m=0}^t \bar{v}_a(\tau_m) \Delta t = \bar{v}_a^\star(t_h)$ and $\sum_{m=0}^t n(\tau_m) \Delta t = w^\star(t_h)$.

Remark 3. In (4.14), the accumulated average of $\bar{v}_a^\star(t_h)$ and $w^\star(t_h)$ can also be considered for all possible filament releasing time.

From (4.14),

$$x_f(t_h) - \bar{v}_a^\star(t_h) = x_s(t_h) + w^\star(t_h). \quad (4.15)$$

The above relationship, (4.15) can be viewed as the information about $x_s(t_h)$ with some noise $w^\star(t_h)$. Hence,

$$q_i(t_h) = x_s(t_h) + w^\star(t_h). \quad (4.16)$$

Therefore, ϕ in (4.3) can now be constructed from (4.7) & (4.16).

Trajectory mapping for the leader agent

The detection of information of interest based on instantaneous sensing of plume depends on the threshold value of sensors, and the next state is decided according to this threshold. Hence, the blueprints of trajectory planning can be described in terms of following behavior.

- **Surging:** If the i^{th} agent receives data well above threshold, we say that some clues about the location of the source have been detected. If the predicted position of the source at $t = t_h$ as seen by i^{th} agent be given as $x_{s_i}(t_h)$, then the next state of the agent is given mathematically as

$$x_i(t_{h+1}) = x_{s_i}(t_h) \quad (4.17)$$

- **Casting:** If the i^{th} agent fails to detect information at any particular instant, then the next state is obtained using the following relation.

$$x_i(t_{h+1}) = \frac{\|x_i(t_h) - x_{s_i}(t_h)\|}{2} + x_{s_i}(t_h) \quad (4.18)$$

- **Search and exploration:** If all the agents fail to detect odor clues for a time segment $[t_h, t_{h+l}] > \delta_0$ for some $l \in \mathbb{N}$ and $\delta_0 \in \mathbb{R}^+$ being the time interval for which no clues are detected or some constraint on wait time placed at the start of the experiment, then the next state is updated as

$$x_i(t_{h+1}) = x_{s_i}(t_h) + F_\sigma^\psi \quad (4.19)$$

In (4.19), F_σ^ψ is some random parameter with σ as its standard deviation and ψ as its mean.

Control protocol for first order agents

In the control layer, we design a robust and powerful controller on the paradigms of sliding mode. It is worthy to mention that based on instantaneous sensing and swarm information, at different times, each agent can take up the role of a virtual leader whose opinion needs to be kept by other agents. The trajectory is planned by the leader agent based on surging, casting and searching behavior.

ϕ from (4.3) has been provided to the controller as the reference to be tracked. The tracking error is formulated as

$$e_i(t) = x_i(t) - \phi(t_h); \quad t \in [t_h, t_{h+1}). \quad (4.20)$$

In terms of graph theory, we can reformulate the error variable as

$$\epsilon_i(t) = (\mathcal{L} + \mathcal{B})e_i(t) = (\mathcal{L} + \mathcal{B})(x_i(t) - \phi(t_h)). \quad (4.21)$$

From this point onward, we shall denote $\mathcal{L} + \mathcal{B}$ as \mathcal{H} . Next, we propose the nonlinear sliding manifold

$$s_i(t) = \lambda_1 \tanh(\lambda_2 \epsilon_i(t)), \quad (4.22)$$

which offers faster reachability to the surface. $\lambda_1 \in \mathbb{R}^+$ represents the speed of convergence to the surface, and $\lambda_2 \in \mathbb{R}^+$ denotes the slope of the nonlinear sliding manifold. These are coefficient weighting parameters that affect the system performance. In linear sliding manifolds, the magnitude of error is directly proportional to the magnitude of control effort needed to maintain sliding motion. In order to prevent violations of actuator constraints, the control effort is hard upper and lower bounded by some finite value, thereby making only a portion of the manifold attractive (termed as sliding regime). There is no guarantee of desired performance or stability outside the sliding regime. Moreover, if the reference state is too far from the current system state and the actuator saturates, the controller is unable to cope up, resulting in instability. Hence, it is beneficial to design nonlinear sliding manifolds that can hold the system states regardless of their location in the state space.

The forcing function has been proposed as

$$\dot{s}_i(t) = -\mu \sinh^{-1}(m + w|s_i(t)|)sign(s_i(t)). \quad (4.23)$$

In (4.23), m is a small offset such that the argument of $\sinh^{-1}(\cdot)$ function remains non zero and w is the gain of the controller. The parameter μ facilitates additional

gain tuning. In general, $m \ll w$. This novel reaching law contains a nonlinear gain and provides faster convergence towards the manifold. Moreover, this reaching law is smooth and chattering free, which is highly desirable in mechatronic systems to ensure safe operation.

Remark 4. The novel reaching law/forcing function in (4.23) that has been used in the synthesis of the controller possesses a nonlinear gain factor and is smooth as opposed to other reaching laws appearing in the literature of sliding mode control. This control protocol (4.32) ensures faster convergence of state trajectories to the sliding manifold depending on the parameters μ and w .

The inverse hyperbolic function is odd & monotonous. $\sinh^{-1}(\cdot)$ increases with increase in its positive argument and decreases with decrease in its negative argument. As its argument value decreases, the value of the function approaches 0. Note that, there is ambiguity in the value of $\sinh^{-1}(\cdot)$ at zero argument. Hence, in order to ascertain that the value of the function never equals 0, the parameter m comes into picture and is used as a small offset.

The time required by the control law to reach the sliding manifold (t_r) can be calculated as follows. Recall from (4.23) that

$$\begin{aligned} \dot{s}_i(t) &= -\mu \sinh^{-1}(m + w|s_i(t)|) \operatorname{sign}(s_i(t)) \\ \therefore -\mu \operatorname{sign}(s_i(t)) dt &= \frac{ds_i(t)}{\sinh^{-1}(m + w|s_i(t)|)} \\ \Rightarrow \int_0^{t_r} dt &= \frac{1}{\mu} \int_0^{s_i(0)} \frac{\operatorname{sign}(s_i(t))}{\sinh^{-1}(m + w|s_i(t)|)} ds_i(t) \end{aligned} \quad (4.24)$$

For $\operatorname{sign}(s_i(t)) > 0$, we have

$$\int_0^{t_r} dt = \frac{1}{\mu} \int_0^{s_i(0)} \frac{ds_i(t)}{\sinh^{-1}(m + w|s_i(t)|)}. \quad (4.25)$$

For $\operatorname{sign}(s_i(t)) < 0$, we have

$$\int_0^{t_r} dt = -\frac{1}{\mu} \int_0^{s_i(0)} \frac{ds_i(t)}{\sinh^{-1}(m + w|s_i(t)|)} = \frac{1}{\mu} \int_0^{-s_i(0)} \frac{ds_i(t)}{\sinh^{-1}(m + w|s_i(t)|)}. \quad (4.26)$$

From (4.25, 4.26), the results can be combined as

$$\int_0^{t_r} dt = \frac{1}{\mu} \int_0^{|s_i(0)|} \frac{ds_i(t)}{\sinh^{-1}(m + w|s_i(t)|)} \quad (4.27)$$

which can be further simplified as

$$t_r = \frac{1}{\mu} \int_0^{|s_i(0)|} \frac{ds_i(t)}{\sinh^{-1}(m + w|s_i(t)|)}. \quad (4.28)$$

$$\therefore t_r = \frac{1}{\mu w} \left(\chi(\sinh^{-1}(m + w|s_i(0)|)) - \chi(\sinh^{-1}(m)) \right) \quad (4.29)$$

where $\chi(\cdot)$ denotes the *cosh integral* function. By definition,

$$\chi[z] = \gamma + \text{Ln}[z] + \int_0^z \frac{\cosh(t) - 1}{t} dt \quad (4.30)$$

with $\gamma = 0.577216$ as the Euler's constant.

$$\text{Thus, } t_r \propto \frac{1}{\mu w}. \quad (4.31)$$

Hence, higher the gain parameters, lesser the convergence time.

Theorem 4.4.1. *Given the dynamics of multi-agent systems (4.1) connected in a directed topology, error candidates (4.20, 4.21) and the sliding manifold (4.22), the stabilizing control law that ensures accurate reference tracking under consensus can be described as*

$$u_{SM_i}(t) = -\{(\Lambda \mathcal{H})^{-1} \mu \sinh^{-1}(m + w|s_i(t)|) \text{sign}(s_i(t)) \Gamma^{-1} + (f(x_i(t)) - \dot{\phi}(t_h))\} \quad (4.32)$$

where $\Lambda = \lambda_1 \lambda_2$, $\Gamma = 1 - \tanh^2(\lambda_2 \epsilon_i(t))$, $w > \sup_{t \geq 0} \{\|s_i\|\}$ & $\mu > \sup\{\|\Lambda \mathcal{H} s_i \Gamma\|\}$.

Remark 5. As mentioned earlier, $\lambda_1, \lambda_2 \in \mathbb{R}^+$. This ensures $\Lambda \neq 0$ and hence its non singularity. The argument of $\tanh(\cdot)$ is always finite and satisfies $\lambda_2 \epsilon_i(t) \neq \pi i (\kappa + 1/2)$ for $\kappa \in \mathbb{Z}$, thus Γ is also invertible. Moreover the non singularity of \mathcal{H} can be established directly if the digraph contains a spanning tree with leader agent as a root (lemma 2.2.2).

Proof. From (4.21) and (4.22), we can write

$$\dot{s}_i(t) = \lambda_1 \{\lambda_2 \dot{\epsilon}_i(t)(1 - \tanh^2(\lambda_2 \epsilon_i(t)))\} \quad (4.33)$$

$$= \lambda_1 \lambda_2 \dot{\epsilon}_i(t) - \lambda_1 \lambda_2 \dot{\epsilon}_i(t) \tanh^2(\lambda_2 \epsilon_i(t)) \quad (4.34)$$

$$= \lambda_1 \lambda_2 \dot{\epsilon}_i(t) \{1 - \tanh^2(\lambda_2 \epsilon_i(t))\} \quad (4.35)$$

$$= \Lambda \mathcal{H}(\dot{x}_i(t) - \dot{\phi}(t_h)) \Gamma \quad (4.36)$$

with Λ & Γ as defined in Theorem 4.4.1. From (4.1), (4.36) can be further simplified as

$$\dot{s}_i(t) = \Lambda \mathcal{H}(f(x_i(t)) + u_{\text{SM}_i}(t) + \varsigma_i - \dot{\phi}(t_h))\Gamma. \quad (4.37)$$

Using (4.23), the control that brings the state trajectories on to the sliding manifold can now be written as

$$u_{\text{SM}_i}(t) = -\{(\Lambda \mathcal{H})^{-1} \mu \sinh^{-1}(m + w|s_i(t)|) \text{sign}(s_i(t)) \Gamma^{-1} + (f(x_i(t)) - \dot{\phi}(t_h))\},$$

which is same as (4.32), thereby completing the proof.

Remark 6. The control (4.32) can be practically implemented as it does not contain the uncertainty term.

The sudden surge of interest in the event-driven design of circuits and systems is due to their enhanced performance in applications where resources are constrained. Synchronous architectures of circuits and systems have been in dominance for a long time but they prove to be sub-optimal in terms of resource utilization. Sampling the signal and transmitting the samples over the communication channel, and at the same time occupying the computational unit when the signal does not vary significantly, are evident waste of resources. In networked control system like multi-agent systems connected over shared network consisting of rapid information exchange between nodes, resources such as bandwidth and processor time are always constrained. The exigent need for the economical use of computational and communication resources becomes indispensable and event-based control is expected to yield better results in such scenario. The controller gets updated only when an event (noticeable change) occurs, thereby significantly minimizing computational requirements and power consumption. Event-based sampling and control is advantageous if the requirement is to execute different task in time shared manner, and also where control is expensive. It is also advantageous in situations when steady state needs to be upper bounded at start regardless of initial conditions and the behaviour of state evolution.

Event based sampling has often been described as an alternative to periodic sampling. Next sample instant is dependent on the triggering of an *event*. Hence, the control protocol (4.32) is executed at $t = t^k$ instants only. Thus, $\forall t \in [t^k, t^{k+1})$, the protocol is

$$u_{\text{SM}_i}(t) = -\{(\Lambda \mathcal{H})^{-1} \mu \sinh^{-1}(m + w|s_i(t^k)|) \text{sign}(s_i(t^k)) \Gamma^{-1} + (f(x_i(t^k)) - \dot{\phi}(t_h))\}. \quad (4.38)$$

The error introduced due to discretization of the protocol (4.38) is

$$\Xi_i = x_i(t^k) - x_i(t). \quad (4.39)$$

It is crucial to analyze the necessary and sufficient conditions for the existence of sliding mode when control protocol (4.38) is used. We regard the system to be in sliding mode if for any time $t_1 \in [0, \infty)$, system trajectories are brought upon the manifold $s_i(t) = 0$ and are constrained there for all time thereafter, i.e., for $t \geq t_1$, sliding motion occurs.

Theorem 4.4.2. *Consider the system described by (4.1), error candidates (4.20, 4.21), sliding manifold (4.22) and the control protocol (4.38). Sliding mode is said to exist in vicinity of sliding manifold, if the manifold is attractive, i.e., trajectories emanating outside it continuously decrease towards it. Stating alternatively, reachability to the surface is ensured for some reachability constant $\eta > 0$. Moreover, stability can be guaranteed in the sense of Lyapunov if gain μ is designed as $\mu > \sup\{\|\Lambda\mathcal{H}\varsigma_i\Gamma\| + \|\Lambda\mathcal{H}\|\bar{L}\|\Xi(t)\|\|\Gamma\|\}$.*

Proof. Let us take into account, a Lyapunov function candidate

$$V_i = 0.5s_i^2. \quad (4.40)$$

Taking derivative of (4.40) along system trajectories yield

$$\dot{V}_i = s_i \dot{s}_i \quad (4.41)$$

$$= s_i \{ \Lambda\mathcal{H}(f(x_i(t)) + u_{SM_i}(t) + \varsigma_i - \dot{\phi}(t_h))\Gamma \}. \quad (4.42)$$

Substituting the control protocol (4.38) in (4.42), we have

$$\begin{aligned} \dot{V}_i &= s_i(t) \left(-\mu \sinh^{-1}(m + w|s_i(t^k)|) sign(s_i(t^k)) + \Lambda\mathcal{H}\varsigma_i\Gamma \right. \\ &\quad \left. + \Lambda\mathcal{H}\{f_i(x_i(t)) - f_i(x_i(t^k))\} \right) \\ &\leq \|s_i(t)\| \left\{ \|\Lambda\mathcal{H}\|\bar{L}\|x_i(t) - x_i(t^k)\|\|\Gamma\| + \|\Lambda\mathcal{H}\varsigma_i\Gamma\| \right. \\ &\quad \left. - \mu \sinh^{-1}(m + w|s_i(t^k)|) sign(s_i(t^k)) \right\} \\ &\leq \|s_i(t)\| \left\{ \|\Lambda\mathcal{H}\|\bar{L}\|\Xi(t)\|\|\Gamma\| + \|\Lambda\mathcal{H}\varsigma_i\Gamma\| \right. \\ &\quad \left. - \mu \sinh^{-1}(m + w|s_i(t^k)|) sign(s_i(t^k)) \right\}. \end{aligned} \quad (4.43)$$

As long as $s_i(t) > 0$ or $s_i(t) < 0$, the criterion $sign(s_i(t)) = sign(s_i(t^k))$ is strictly satisfied $\forall t \in [t^k, t^{k+1}]$. Hence, when state trajectories are just outside in the vicinity

of the manifold,

$$\begin{aligned}\dot{V}_i &\leq \left\{ \|s_i(t)\| \|\Lambda\mathcal{H}\| \|\bar{L}\| \|\Xi(t)\| \|\Gamma\| + \|s_i(t)\| \|\Lambda\mathcal{H}_{\mathcal{S}_i} \Gamma\| \right. \\ &\quad \left. - \mu \sinh^{-1}(m + w|s_i(t^k)|) \|s_i(t)\| \right\} \\ &\leq -\eta \|s_i(t)\|.\end{aligned}\tag{4.44}$$

where $\eta = \mu \sinh^{-1}(m + w|s_i(t^k)|) - \|\Lambda\mathcal{H}_{\mathcal{S}_i} \Gamma\| - \|\Lambda\mathcal{H}\| \|\bar{L}\| \|\Xi(t)\| \|\Gamma\| > 0$ is called reachability constant, and $\mu > \sup\{\|\Lambda\mathcal{H}_{\mathcal{S}_i} \Gamma\| + \|\Lambda\mathcal{H}\| \|\bar{L}\| \|\Xi(t)\| \|\Gamma\|\}$. This shows that the manifold is attractive and trajectories tend to decrease towards it $\forall t \in [t^k, t^{k+1}]$.

To ascertain stability in the sense of Lyapunov, it requires to be proved that $\dot{V}_i < 0$. At instants $t = t^k$, the discretization error (4.39) is nullified. Therefore, when $s_i(t) = 0$ and $t = t^k$, we have

$$\dot{V}_i < 0.\tag{4.45}$$

Thus, the derivative of Lyapunov function candidate is negative definite confirming stability in the sense of Lyapunov. Since, $\mu > 0$, $\|s_i\| > 0$ and $\sinh^{-1}(\cdot) > 0$ due to the nature of its arguments. Therefore, (4.23) and (4.44) together provide implications that $\forall s_i(0)$, $s_i \dot{s}_i < 0$ and the surface is globally attractive. This completes the proof.

The time instants t^k , i.e., instants when an event is triggered are completely characterized by a triggering rule. This rule decides when the controller should be updated with a fresh value. As long as this rule is not violated, next clock pulse is not called upon and the control is held constant between successive sampling instants, i.e, the control is maintained at its previous value until the next sampling instant. We have utilized a novel triggering rule in this research. This triggering is dynamic in nature, depending upon measure of error and its derivative. The acceptable band in which the system can tolerate fluctuations without comprising robustness is also exponential, thereby improving the performance during steady state. The complete triggering rule [30] is given by

$$\rho = \varrho_1 \epsilon_i(t) + \varrho_2 \dot{\epsilon}_i(t)^2 - (\zeta_0 + \zeta_1 e^{-\xi t}).\tag{4.46}$$

In (4.46), $\varrho_1 > 0$, $\varrho_2 > 0$, $\zeta_0 \geq 0$, $\zeta_1 \geq 0$, $\zeta_0 + \zeta_1 > 0$ and $\xi \in (0, \lambda_2(\mathcal{L}))$. Note that $\lambda_2(\mathcal{L})$ denotes the second eigenvalue of the Laplacian matrix when all its eigenvalues are arranged in ascending order.

We shall take $\varrho_1 = 0.8$, $\varrho_2 = 0.6$, $\zeta_0 = 10^{-4}$, $\zeta_1 = 0.2278$ and $\xi = 0.57$ during the synthesis process.

Named after the ancient Greek philosopher *Zeno* of Elea, *Zeno* phenomenon is unique to hybrid systems, and represents the occurrence of infinite number of events in a finite time segment. Stated alternately, the systems undergoes an unbounded number of discrete transitions in a bounded and finite time segment. The purpose of reducing the communication burden in a hybrid system is defeated if this phenomenon occurs in the system. This can lead to prevention of existence of global solutions to be defined for all time. In order to prevent the accumulation of samples at the same time, it is necessary to ensure that adjacent samples are separated in time by a small finite quantity, thereby ensuring a positive lower bound on inter-event execution time. This finite lower bound has to be carefully checked, and has been derived here to ensure that the system is Zeno-free.

Theorem 4.4.3. *Consider the system presented in (4.1), the control protocol (4.38), and the discretization error 4.39). The sequence of triggering instants $\{t_i^k\}_{k=0}^\infty$ respects the triggering rule 4.46). The inter-event execution time T_i^k is lower bounded by a finite positive quantity ϖ such that $T_i^k \geq \varpi$, where*

$$\varpi = \frac{1}{L} \ln \left(1 + \frac{\|\Xi_i(t)\|_\infty}{\Omega(\|x_i(t^k)\|) + \|\dot{\phi}(t_h)\| + \varkappa} \right). \quad (4.47)$$

As a consequence, accumulation of samples at the same instant, i.e., Zeno phenomenon is excluded.

Proof. Between k^{th} and $(k+1)^{th}$ sampling instant in the execution of control, the discretization error is non zero. $T_i^k = t_i^{k+1} - t_i^k$ is the time it takes the discretization error to rise from 0 to $\|\Xi_i\|_\infty$. Thus,

$$\begin{aligned} \frac{d}{dt} \|\Xi_i(t)\| &\leq \left\| \frac{d}{dt} \Xi_i(t) \right\| \leq \left\| \frac{d}{dt} x_i(t) \right\| \\ \Rightarrow \left\| \frac{d}{dt} \Xi_i(t) \right\| &\leq \|f(x_i(t)) + u_{SM_i} + \varsigma_i\| \end{aligned} \quad (4.48)$$

Substituting the control protocol (4.38) in the inequality (4.48), we have

$$\begin{aligned}
\left\| \frac{d}{dt} \Xi_i(t) \right\| &\leq \| -(\Lambda \mathcal{H})^{-1} \mu \sinh^{-1}(m + w|s_i(t^k)|) sign(s_i(t^k)) \Gamma^{-1} \\
&\quad + f(x_i(t)) - f(x_i(t^k)) + \varsigma_i \dot{\phi}(t_h) \| \\
&\leq \bar{L} \|x_i(t)\| + \bar{L} \|x_i(t^k)\| + \|\varsigma_i\| + \|\dot{\phi}(t_h)\| \\
&\quad + \|(\Lambda \mathcal{H})^{-1} \mu \sinh^{-1}(m + w|s_i(t^k)|)\| \|\Gamma^{-1}\| \\
&\leq \bar{L} \|x_i(t^k) + \Xi_i(t)\| + \bar{L} \|x_i(t^k)\| + \|\varsigma_i\| + \|\dot{\phi}(t_h)\| \\
&\quad + \|(\Lambda \mathcal{H})^{-1} \mu \sinh^{-1}(m + w|s_i(t^k)|)\| \|\Gamma^{-1}\| \\
&\leq \bar{L} \|\Xi_i(t)\| + 2\bar{L} \|x_i(t^k)\| + \|\varsigma_i\| + \|\dot{\phi}(t_h)\| \\
&\quad + \|(\Lambda \mathcal{H})^{-1} \mu \sinh^{-1}(m + w|s_i(t^k)|)\| \|\Gamma^{-1}\| \\
&\leq \bar{L} \|\Xi_i(t)\| + \Omega(\|x_i(t^k)\|) + \varkappa + \|\dot{\phi}(t_h)\|. \tag{4.49}
\end{aligned}$$

In (4.49), $\Omega(\|x_i(t^k)\|) = 2\bar{L} \|x_i(t^k)\|$, $\varkappa = \|(\Lambda \mathcal{H})^{-1} \mu \sinh^{-1}(m + w|s_i(t^k)|)\| \|\Gamma^{-1}\| + \|\varsigma_i\|$ and $\|\dot{\phi}(t_h)\|$ are all positive quantities. The solution to the differential inequality of (4.49) $\forall t \in [t^k, t^{k+1})$ can be understood by incorporating Comparison Lemma [75] with initial condition $\|\Xi_i(t^k)\| = 0$. Thus,

$$\|\Xi_i(t)\| \leq \frac{\Omega(\|x_i(t^k)\|) + \|\dot{\phi}(t_h)\| + \varkappa}{\bar{L}} \left(e^{\bar{L}(t_i - t_i^k)} - 1 \right) \tag{4.50}$$

The triggering rule (4.46) can be defined in an iterative manner as

$$t_i^{k+1} = \inf\{t_i^k \in [t_i^k, \infty) : \rho > 0\}. \tag{4.51}$$

Hence, at instant $t = t^{k+1}$, we have

$$\|\Xi_i(t)\|_\infty = \|\Xi_i(t^{k+1})\| \leq \frac{\Omega(\|x_i(t^k)\|) + \|\dot{\phi}(t_h)\| + \varkappa}{\bar{L}} \left(e^{\bar{L}T_i^k} - 1 \right). \tag{4.52}$$

Computing T_i^k from (4.52), gives

$$T_i^k \geq \frac{1}{\bar{L}} \ln \left(1 + \frac{\|\Xi_i(t)\|_\infty}{\Omega(\|x_i(t^k)\|) + \|\dot{\phi}(t_h)\| + \varkappa} \right), \tag{4.53}$$

which is same as ϖ given in (4.47). Comparison Lemma is particularly useful when information on bounds on the solution [75, 76] is more crucial than the solution itself. Thus, from (4.52), it can be inferred that there is a finite positive lower bound on the inter-event execution time, and the triggers are admissible. This concludes the proof.

RESULTS OF NUMERICAL SIMULATION

The sense of smell, like a faithful counsellor, foretells its character.

Jean Anthelme Brillat-Savarin

Interaction topology of the agents [77] represented as a digraph has been shown here in figure 5.1. The associated graph matrices have been described below. Computer simulations have been performed assuming that agent 1 appears as virtual leader to all other agents, making the topology fixed and directed for this study. It should be noted that, the theory developed so far can be extended to the case of switching topology and shall be dealt in future.

Assumption 5.0.1. *Agent 1 appears as the virtual leader to all other agents. Therefore, the topology is fixed and directed.*

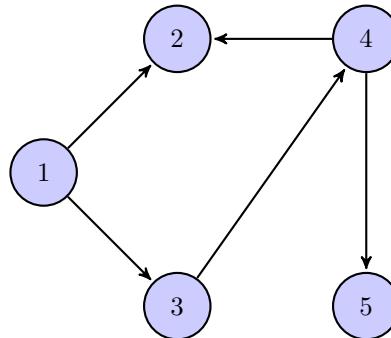


Figure 5.1: Interaction topology of agents

$$\mathcal{A} = \begin{bmatrix} 0 & 0 & 1 & 0 \\ 0 & 0 & 0 & 0 \\ 0 & 1 & 0 & 0 \\ 0 & 0 & 1 & 0 \end{bmatrix}, \quad \mathcal{B} = \begin{bmatrix} 1 & 0 & 0 & 0 \\ 0 & 1 & 0 & 0 \\ 0 & 0 & 0 & 0 \\ 0 & 0 & 0 & 0 \end{bmatrix}, \quad \mathcal{D} = \begin{bmatrix} 1 & 0 & 0 & 0 \\ 0 & 0 & 0 & 0 \\ 0 & 0 & 1 & 0 \\ 0 & 0 & 0 & 1 \end{bmatrix},$$

$$\mathcal{L} = \mathcal{D} - \mathcal{A} = \begin{bmatrix} 1 & 0 & -1 & 0 \\ 0 & 0 & 0 & 0 \\ 0 & -1 & 1 & 0 \\ 0 & 0 & -1 & 1 \end{bmatrix}, \quad \mathcal{L} + \mathcal{B} = \begin{bmatrix} 2 & 0 & -1 & 0 \\ 0 & 1 & 0 & 0 \\ 0 & -1 & 1 & 0 \\ 0 & 0 & -1 & 1 \end{bmatrix}. \quad (5.1)$$

Odor molecules tend to disperse heavily in the environment characterized by diffusion. In making assumption of a diffusion dominated environment, several factors are ignored. A more realistic picture must include effects of wind, turbulence diffusion and thermal effects. However, effects of turbulence are difficult to be described mathematically. In addition to the effects of wind, the characteristics of environment can also be described by advection phenomenon. Hence, we have considered a diffusion-advection plume model in our discussed source localization problem. Before we begin to use this model, following assumptions need to be stated.

Assumption 5.0.2. *We assume uniform airflow velocity for all time and throughout the domain in which the task of source localization is being performed.*

Assumption 5.0.3. *The turbulence diffusion coefficient K needs to be known beforehand via some suitable measurements. In case K is not known beforehand, then K should be estimated or correlated as a function of wind velocity, i.e., $K = f(v_a)$. This estimation can be performed during the experiment with the data obtained by sensors (e.g. anemometers, gas sensors).*

The diffusion-advection model provided [78, 79] has been recalled here to simulate the dynamic plume under time varying disturbances. Initial conditions have been chosen to be far from the equilibrium point. We shall consider a time varying disturbance $\zeta_i = 0.3 \sin(\pi^2 t^2)$ for matched case and $\zeta_i = 20 \sin(\pi^2 t^2)$ for mismatched case, accuracy parameter $\theta = 0.001$ and maximum mean airflow velocity $\bar{v}_{a_{max}} = 1$ m/s. Other key design parameters are provided in table 5.1.

Table 5.1: Values of the design parameters used in simulation

k_1	ω_{max}	α_1	α_2	λ_1	λ_2	μ	m	w
0.5	2 rad/s	0.25	0.25	1.774	2.85	5	10^{-3}	2

A steady concentration profile for a very large span of time ($t \rightarrow \infty$) can be written as

$$C(\vec{r}, \infty) = \frac{q_0}{2\pi K d_i} \exp \left\{ -\frac{v_a}{2K} (d_i - \vec{r} + \vec{r}_0) \right\}. \quad (5.2)$$

In (5.2), $\vec{r}_0 = x_s(t)$ represents the coordinates of the odor source, $d_i = \|x_i - x_s\|$, q_0 is the filament release rate and K is the turbulent diffusion coefficient that is independent of the diffusing material. K is taken to be $0.02 \text{ m}^2/\text{sec}$ and $q_0 = 2 \text{ mg/sec}$ of diffusing substance. We shall present the results for both the cases of localization in \mathbb{R}^1 and \mathbb{R}^2 to demonstrate the efficiency of the designed control scheme.

5.1 Source seeking by homogeneous agents

The set of homogeneous agents are described by same dynamics, which has been taken as

$$\dot{x}_i = 0.1 \sin(x_i(t)) + \cos(2\pi t) + u_{SM_i}(t) + \varsigma_i; \quad i \in [1, 5] \in \mathbb{N}. \quad (5.3)$$

Figure 5.2 shows agents coming to consensus in finite time to locate the source of odor. Initial position of the agents are far from origin and have been depicted on the left vertical axis. Similarly, position of the source has been referenced by the right vertical axis. As time progresses, agents move towards the source on the right and come to a consensus as soon as agent 1 (designated as leader in this experiment) acquires information of the plume through equipped sensors. The information of the plume is obtained by sensing the dispersed odor filaments released from the odor source. In figure 5.2, the black dots correspond to the odor filaments that originate at the source (depicted by a gray circle) and travel from right to left. Figure 5.3 depicts agents keeping parallel formation and locating the odor source. In parallel formation, adjacent agents maintain a constant separation between them throughout the localization. From figures 5.2 and 5.3, it can be seen that the agents come to consensus quickly and complete the odor source localization in finite time. The tracking controller tries to minimize the error between the predicted next state and the actual next state. Norms of tracking errors in \mathbb{R}^1 have been shown in figure 5.4a. It is clear that the errors lie in close vicinity of zero, which is expected of such controller. Figure 5.4b is the plot of sliding manifolds during consensus in \mathbb{R}^1 . As soon as consensus is established, the sliding variables converge to the origin in finite time. Note that this convergence is quite fast, and by tailoring the design parameters carefully, one may obtain the desired convergence speed. In fact, nonlinear sliding manifolds prove to be advantageous over linear ones. In linear sliding manifolds, the magnitude of error is directly proportional to the magnitude of control effort needed to maintain sliding motion. In order to satisfy actuator constraints, the control effort is upper and lower bounded by some finite value, thereby making only a part of

the sliding manifold attractive (termed as sliding regime). There is no guarantee of desired performance or stability outside the sliding regime. Moreover, if the reference state is too far from the current system state and the actuator saturates, the controller is unable to cope up, resulting in instability. Hence, it is beneficial to design nonlinear sliding manifolds that can hold the system states regardless of their location in the phase plane.

The control signals using the proposed control is smooth and the signals also come to consensus in finite time. This smoothness of control is highly desirable in mechatronic systems. Traditional sliding mode control utilizes discontinuous control, which is feasible in fast switching circuitry but mechanical systems may result in wear and tear, high heat losses, etc. Due to such nature of the control, their efficiency degrades and operational lifetime reduces. Using inverse sine hyperbolic reaching law, the switching control has been made continuous and smooth without sacrificing the robustness of sliding mode control. Figures 5.5a to 5.5e depict the sampling intervals of each agent under event-based sampling, from where it can be seen that sampling is not uniform. Only a few samples are taken, thus reducing the energy expenses and computational requirements. The total number of controller updates has been tabulated in table 5.4. Figure 5.5f depicts the smooth control signals for the case of \mathbb{R}^1 during localization via consensus.

To further aid the proposition and to illustrate the efficiency of the synthesized control, 50 repeated trials were conducted for four cases. In each trial the initial conditions were varied keeping the design parameters fixed. The statistics have been shown in figure 5.6 for time-based and event-based control. The four cases considered have been provided in a tabular format in table 5.2. Case 1 corresponds to localization by making a group consensus without influence of any disturbance. Case 2 corresponds to localization by making a parallel formation under the absence of disturbances. Cases 3 and 4 respectively represent localization via consensus, and parallel formation under the influence of matched and bounded disturbance, i.e., disturbances that enter the system through the same channel as the control, and lie in the range space of the input matrix.

For each case mentioned in table 5.2, the success rate, median localization time and the control implementation have been tabulated in table 5.3. It is evident that the localization is completed in lesser time in contrast to the time consumed in localization in other studies.

To avoid confusion between state variable x and axis labeled as x in the usual

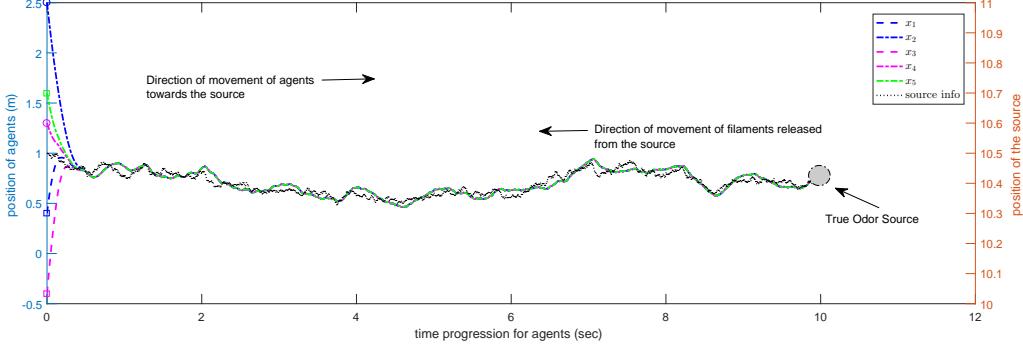


Figure 5.2: Homogeneous agents in consensus to locate source of odor in \mathbb{R}^1

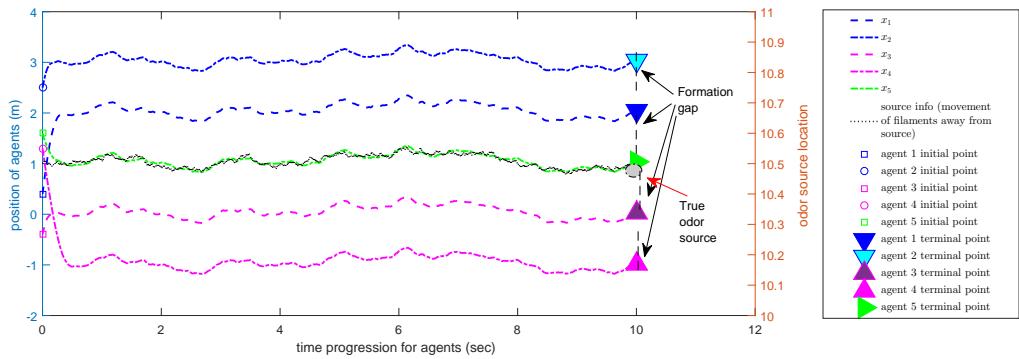


Figure 5.3: Homogeneous agents in formation to locate source of odor in \mathbb{R}^1

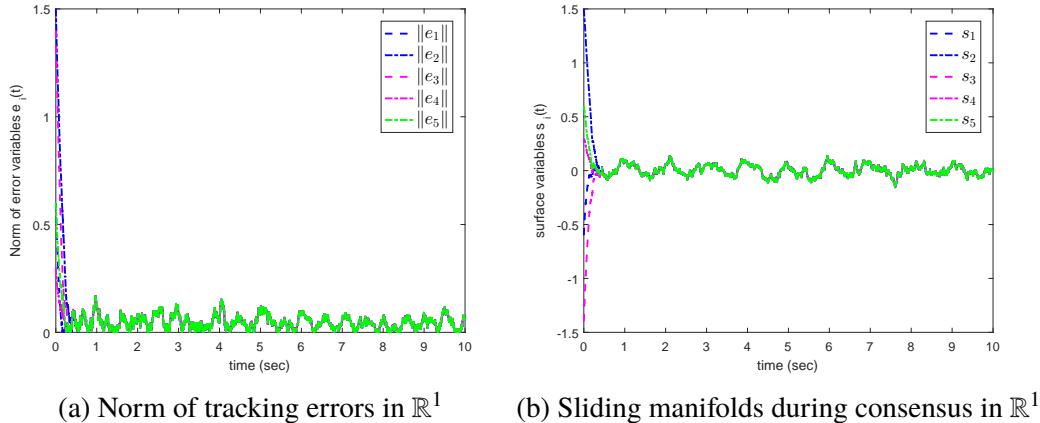


Figure 5.4: Tracking errors and sliding manifolds in \mathbb{R}^1 during localization via consensus (in context of homogeneous agents)

sense, we have designated abscissa as first axis and ordinate as second axis in our discussion. Similar to figure 5.4a, in \mathbb{R}^2 , norms of tracking error variables along first and second axis have been depicted in figures 5.7a and 5.7b respectively. Once again, it is evident that the error is minimal. Complete elimination of error is not

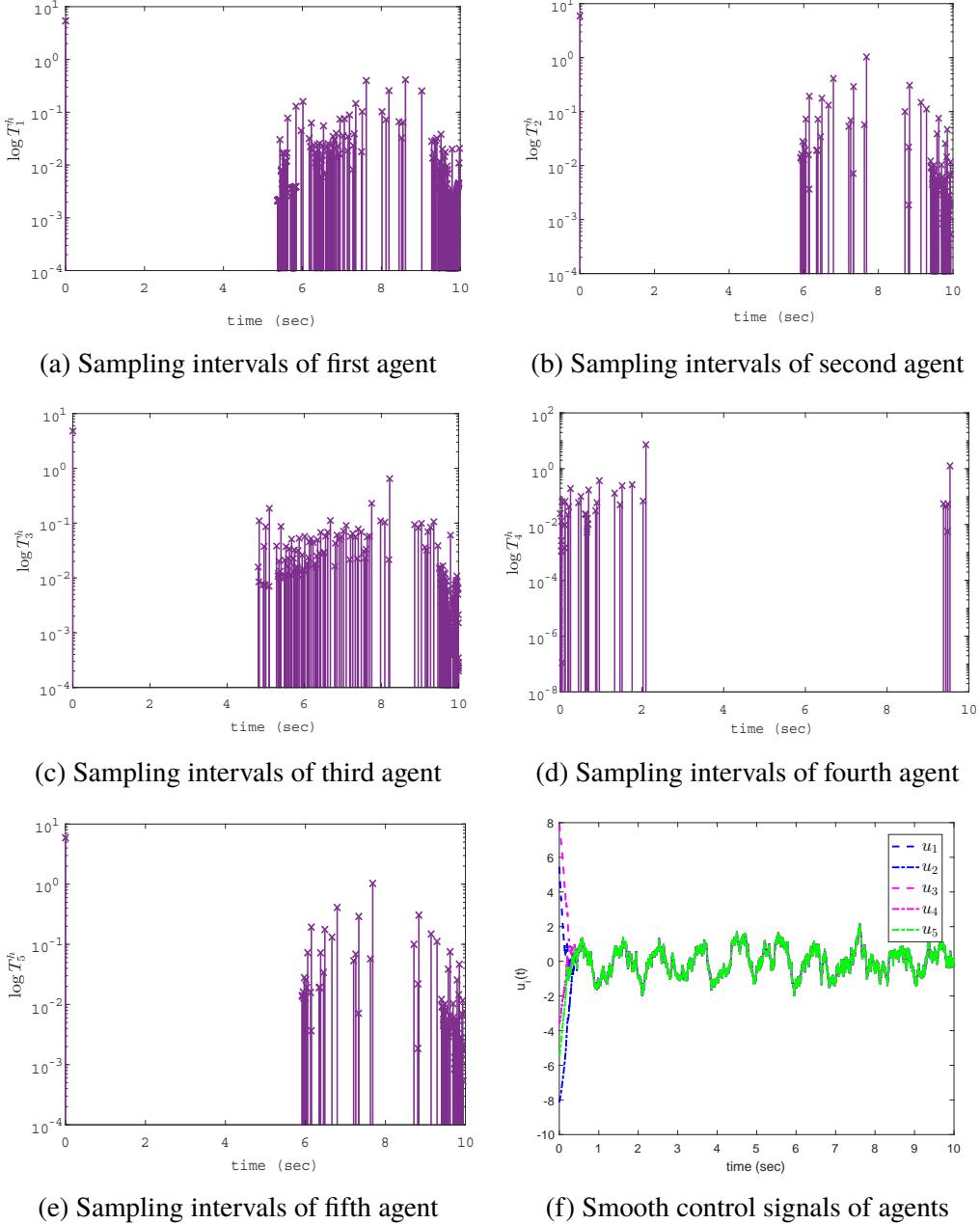
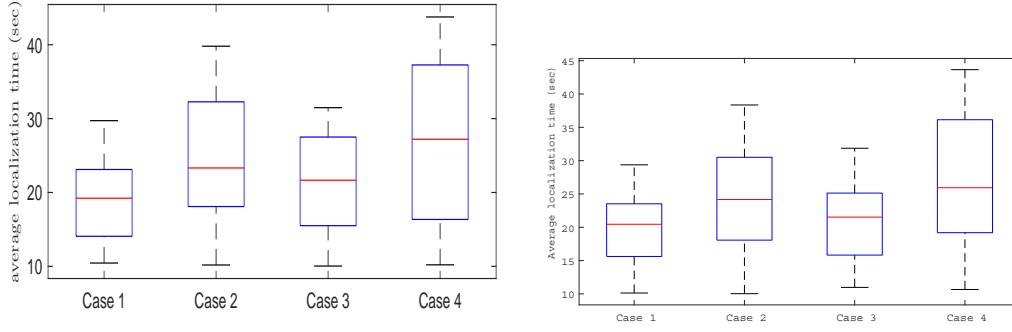


Figure 5.5: Sampling intervals of homogeneous agents and the smooth control signal during consensus

possible because the agents progress towards the source under less than complete information. However, with robust control protocols, the error has been confined to a small vicinity of zero, depicting accurate tracking. Figure 5.8 illustrates agents coming in consensus to locate source of odor in \mathbb{R}^2 . It is evident that state trajectories start from spread out initial conditions and ultimately come to consensus in finite time to locate the odor source. Figure 5.9 shows the case when agents make parallel



(a) Average localization time under time-triggered control (b) Average localization time under event-triggered control

Figure 5.6: Average time consumed by homogeneous agents under time-triggered and event-triggered controls for 50 repeated trials

Table 5.2: Four cases of localization by set of homogeneous agents

Case	Group Consensus	Parallel Formation	No perturbation	Matched perturbations
Case 1	✓	✗	✓	✗
Case 2	✗	✓	✓	✗
Case 3	✓	✗	✗	✓
Case 4	✗	✓	✗	✓

Table 5.3: Performance metrics in context of localization by homogeneous agents

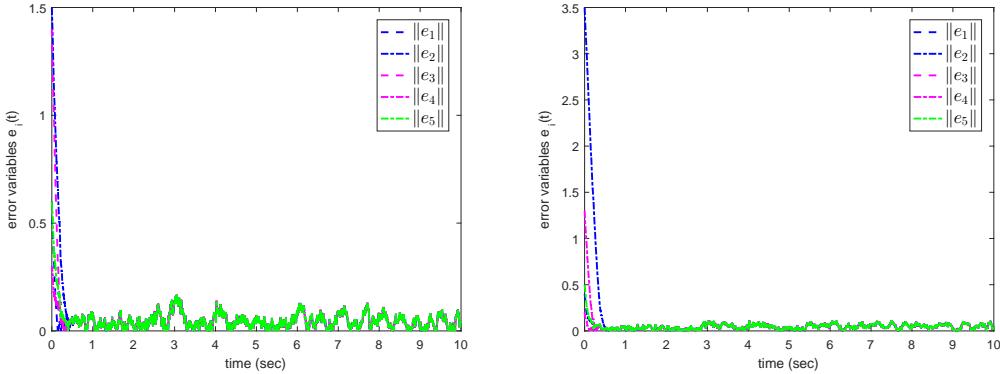
Technique	Average Success rate	Median localization Time	Control Implementation
Case 1 (this study)	100%	19.00 sec	Time-triggered
Case 2 (this study)	100%	22.70 sec	Time-triggered
Case 3 (this study)	100%	21.50 sec	Time-triggered
Case 4 (this study)	100%	28.00 sec	Time-triggered
Case 1 (this study)	100%	21.50 sec	Event-triggered
Case 2 (this study)	100%	24.10 sec	Event-triggered
Case 3 (this study)	100%	22.00 sec	Event-triggered
Case 4 (this study)	100%	26.00 sec	Event-triggered
PSO [68]	21.5%	986.25 sec	Time-triggered
FTMCS [73]	100%	137.50 sec	Time-triggered

Table 5.4: Number of controller updates in the set of homogeneous agents under event-based control law

Agent	Agent 1	Agent 2	Agent 3	Agent 4	Agent 5
No. of controller updates	142	56	188	47	71
Total number of controller updates					504

formation to locate the source in \mathbb{R}^2 . In both the cases, the domain in which odor

source localization has been carried out is depicted by the limits of first and second axes.



(a) Norm of tracking errors along first axis (b) Norm of tracking errors along second axis

Figure 5.7: Norm of tracking errors along both axes in \mathbb{R}^2 (in context of homogeneous agents)

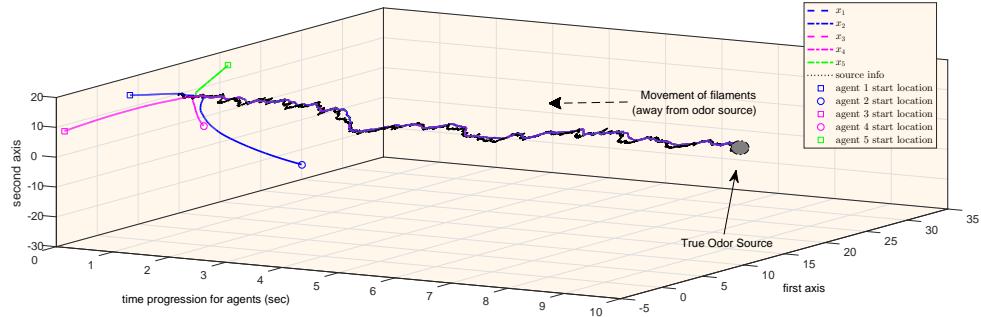


Figure 5.8: Homogeneous agents in consensus to locate source of odor in \mathbb{R}^2

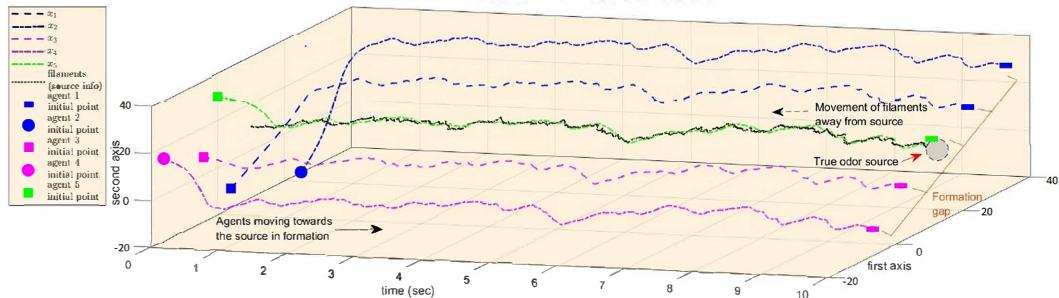


Figure 5.9: Homogeneous agents in formation to locate source of odor in \mathbb{R}^2

5.2 Source seeking by heterogeneous agents

The set of heterogeneous agents are described by non-identical dynamics. The dynamics of heterogeneous agents considered here are

$$\dot{x}_1 = 0.1 \sqrt[3]{\sin(x_1)} + \cos(2\pi t) + u_{SM_1}(t) + \varsigma_1, \quad (5.4)$$

$$\dot{x}_2 = 0.1 \sin(x_2) - \cos(e^{-x_2 t}) + u_{SM_2}(t) + \varsigma_2, \quad (5.5)$$

$$\dot{x}_3 = 0.1 \sqrt[3]{\sin(x_3)} + \cos^2(2\pi t) + u_{SM_3}(t) + \varsigma_3, \quad (5.6)$$

$$\dot{x}_4 = 0.1 \sin(x_4) + \cos(x_4) + u_{SM_4}(t) + \varsigma_4, \quad (5.7)$$

$$\dot{x}_5 = 0.1 \cos(x_5) - \cos(2\pi t) - e^{-t} + u_{SM_5}(t) + \varsigma_5. \quad (5.8)$$

For the case of \mathbb{R}^1 , the odor source is randomly placed between 10 m and 11 m, as shown in figure 5.10. Agents and their respective trajectories are represented by five different colours. The odor source is represented by a gray circle, and the filaments released from the odour source are represented as black dots. Agents start from various initial conditions that are far from the origin. Reference for agents is taken from left hand vertical axis and that for the source is taken from right hand vertical axis. Agents start moving from left hand side to progress towards the source via instantaneous plume sensing (by sensing odor molecules, or filaments). As soon as the leader agent senses the odor molecules, the information of predicted next state is exchanged among other agents. This local information is then used to make a consensus while localization. It is evident that agents come to consensus in finite time to locate the odor source. In spite of time varying disturbance, the plume tracking is accurate and the localization is successful. In figure 5.11, agents locate the odor source in parallel formation. During parallel formation, a fixed distance is maintained between two consecutive agents. In both the cases, filaments or odor molecules (source information) are released from the odor source and are detected by the sensors equipped with the agents. Although the filaments disperse throughout the domain, only the source information relevant to the agents has been shown in the figure. The agents start from left and progress towards the source to the right. The tracking controller attempts to minimize the error between the predicted next state and the actual next state. The tracking error lies in the close vicinity of zero as expected, implying that the tracking error has almost been nullified. Norm of tracking errors in \mathbb{R}^1 has been depicted in figure 5.12a to depict near nullification of error. Sliding manifolds, which has been designed to be novel in this study, also come to consensus in very short span of time, as evident from figure 5.12b. It is, then, quite clear that the convergence of state trajectories to the sliding manifold is very fast, and is highly desired to ensure a high degree of robustness and autonomy.

Such manifolds can also be utilized to attain a desired convergence speed by simple tuning of design parameters.

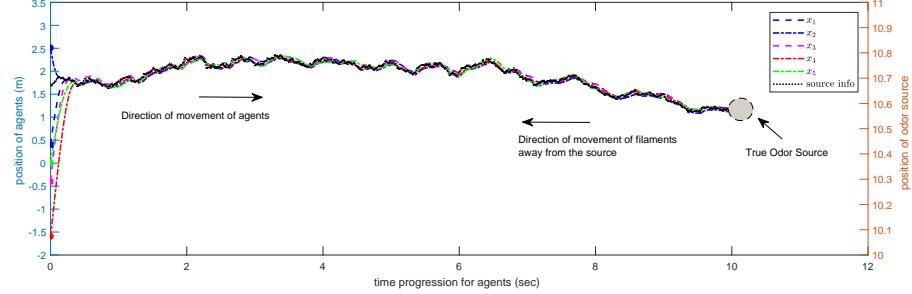


Figure 5.10: Heterogeneous agents in consensus to locate source of odor in \mathbb{R}^1

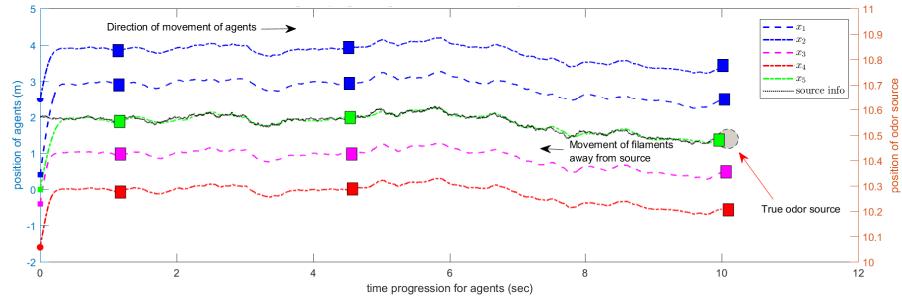


Figure 5.11: Heterogeneous agents in formation to locate source of odor in \mathbb{R}^1

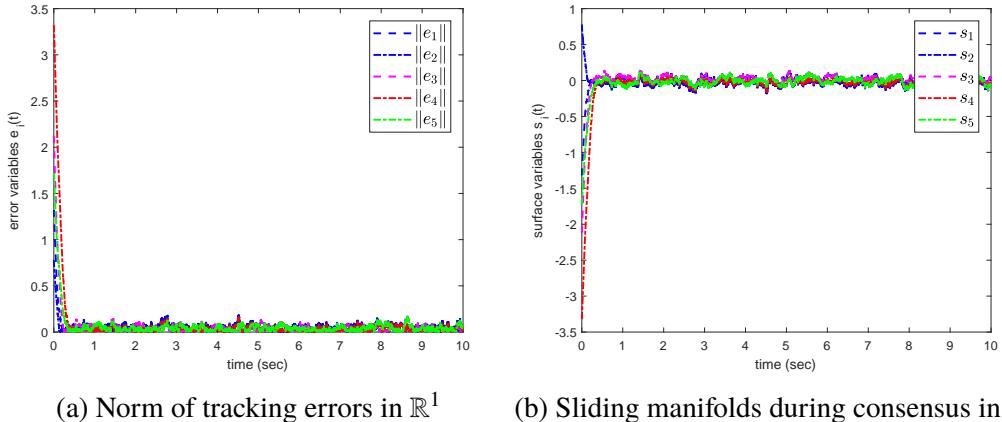


Figure 5.12: Tracking errors and sliding manifolds in \mathbb{R}^1 during localization via consensus (in context of heterogeneous agents)

Under event-based control protocol, non-uniform sampling intervals have been depicted in figures 5.13a- 5.13e. The number of controller updates are more than those for homogeneous agents (see table 5.7). Use of a novel inverse sine hyperbolic reaching law results in a smooth control signals for all the agents. The use of smooth

sliding mode controller ensures safe operation in mechatronic devices. Figure 5.13f depicts the control signals of all the agents when localization is performed in \mathbb{R}^1 . It can be seen that the signal is chattering free, smooth and accurate.

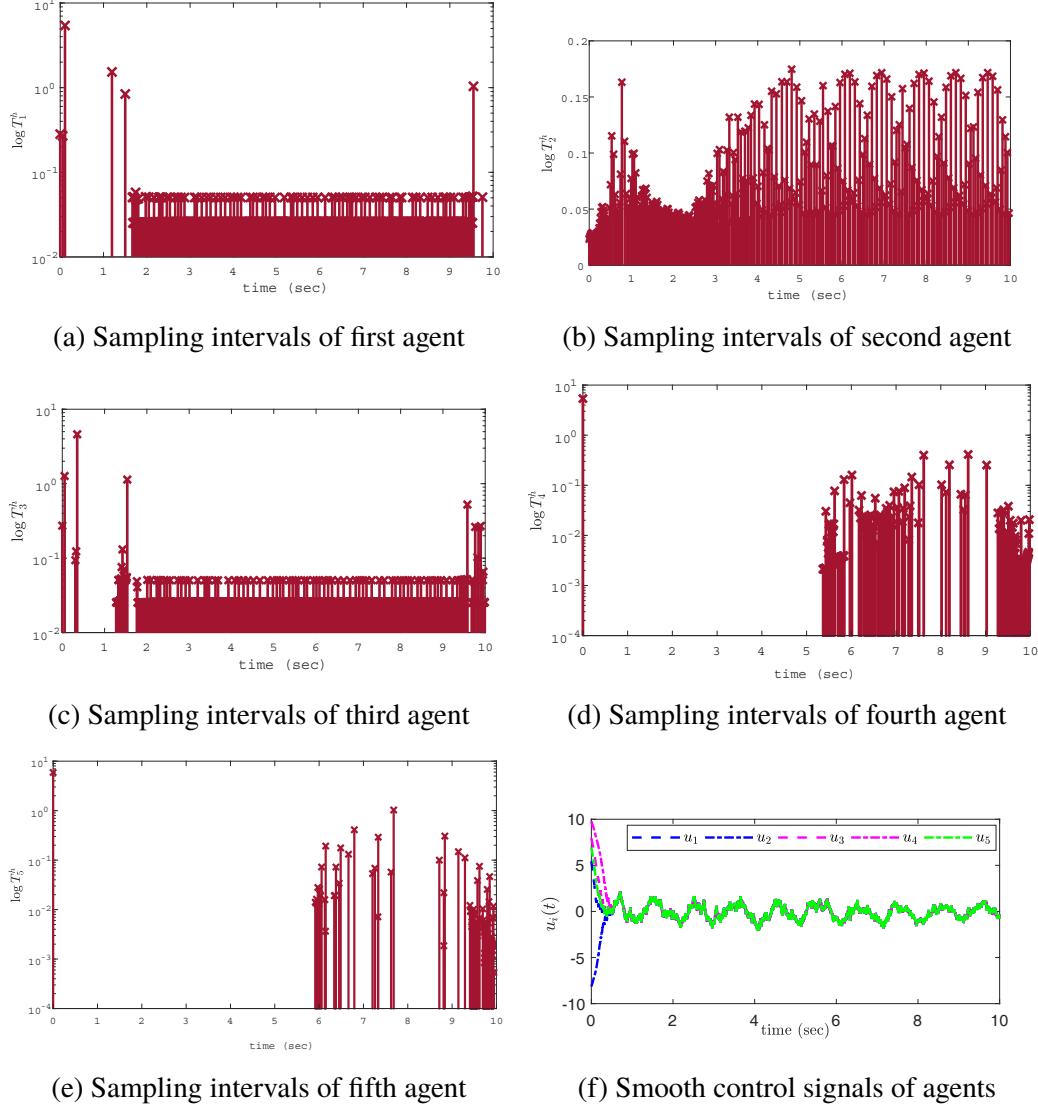


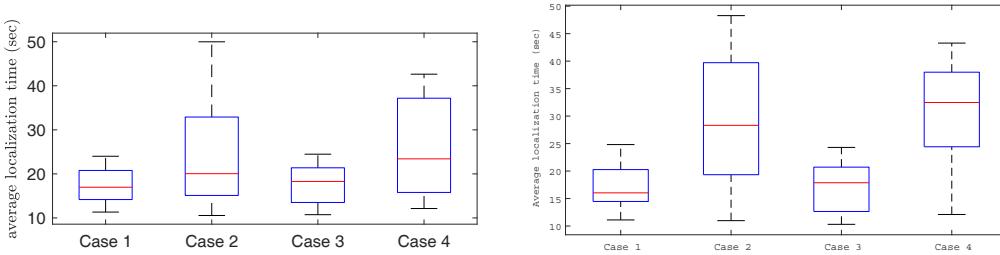
Figure 5.13: Sampling intervals of heterogeneous agents and the smooth control signal during consensus

Having discussed the case of \mathbb{R}^1 , we shall now discuss the odor source localization in \mathbb{R}^2 . To avoid confusion between state variable x and axis labelled as x in the usual sense, we have adopted to refer abscissa as first axis and ordinate as second axis throughout this discussion. Agents are driven into consensus to locate the odor source in \mathbb{R}^2 in the domain described by the axis limits. Within the domain of localization, a total of 25 trials were done with various initial conditions chosen

far from the origin. Figure 5.14 shows the average time spent in four cases under both time-triggered and event-triggered control laws— localization via consensus under matched perturbations (Case 1), localization via formation under matched perturbations (Case 2), localization via consensus under mismatched perturbations (Case 3), and localization via formation under mismatched perturbations (Case 4). Similar to the results in [73], the success rate of this technique is also 100% except for the fact that time spent in localization is lesser via this technique owing to faster convergence of state trajectories to the sliding manifold. The four cases have been illustrated here in a tabular format in table 5.5 for ease of reference. A check (cross) mark in a particular column indicates that the particular strategy has been used (not used) in localization.

Table 5.5: Four cases of localization via set of heterogeneous agents

Technique	Consensus	Formation	Matched perturbations	Mismatched perturbations
Case 1	✓	✗	✓	✗
Case 2	✗	✓	✓	✗
Case 3	✓	✗	✗	✓
Case 4	✗	✓	✗	✓



(a) Average localization time under time-triggered control (b) Average localization time under event-triggered control

Figure 5.14: Average time consumed by heterogeneous agents under time-triggered and event-triggered controls for 25 repeated trials

We shall also present two cases under which localization has been tasked— under consensus and under parallel formation. Note that agents may be subjected to any geometrical pattern, or formation that deems suitable for the task at hand. For a random trial, figure 5.15 shows localization in a turbulent environment under the effect of both mismatched and matched disturbances. Under mismatched disturbances and turbulence, localization takes slightly more time as compared with its matched

Table 5.6: Performance metrics in context of localization by heterogeneous agents

Technique	Average Success rate	Median localization Time	Control Implementation
Case 1 (this study)	100%	16.00 sec	Time-triggered
Case 2 (this study)	100%	20.00 sec	Time-triggered
Case 3 (this study)	100%	18.00 sec	Time-triggered
Case 4 (this study)	100%	22.00 sec	Time-triggered
Case 1 (this study)	100%	19.00 sec	Event-triggered
Case 2 (this study)	100%	22.68 sec	Event-triggered
Case 3 (this study)	100%	21.51 sec	Event-triggered
Case 4 (this study)	100%	28.00 sec	Event-triggered
PSO [68]	21.5%	986.25 sec	Time-triggered
FTMCS [73]	100%	137.50 sec	Time-triggered

Table 5.7: Number of controller updates in the set of heterogeneous agents under event-based control law

Agent	Agent 1	Agent 2	Agent 3	Agent 4	Agent 5
No. of controller updates	271	425	268	104	88
Total number of controller updates					
	1156				

disturbance counterpart. Figure 5.16 depicts wind turbulence in the domain during localization via consensus. Snapshots in four segments of time have been taken, as described in figure 5.16. The first snapshot is taken randomly between $0 < t < 2.5$ sec and the velocity plot depicting turbulence at that time has been presented. Wind turbulence for the case of localization via formation has been illustrated by velocity plots in figure 5.17 similar to that in figure 5.16. In figure 5.18, norms of tracking

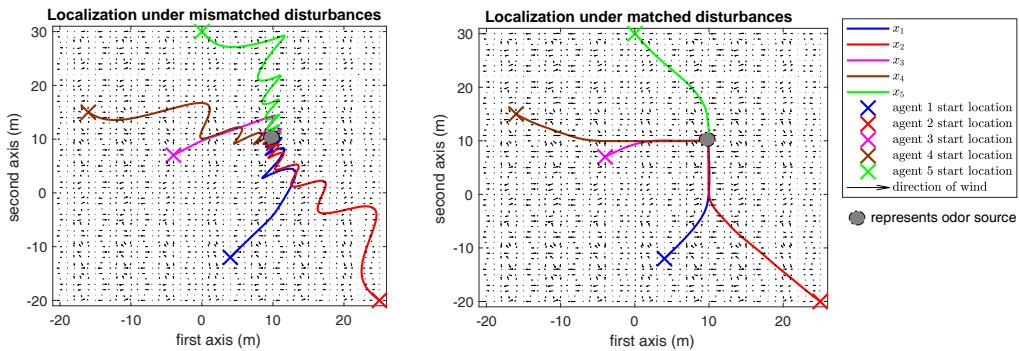


Figure 5.15: Localization by heterogeneous multi-agent systems under the effect of mismatched and matched disturbances

error candidates along first and second axis have been depicted. Similar to the error profile in figure 5.12a, the tracking is accurate and the agents are able to complete the localization task in finite time. Two best case scenarios have been also presented

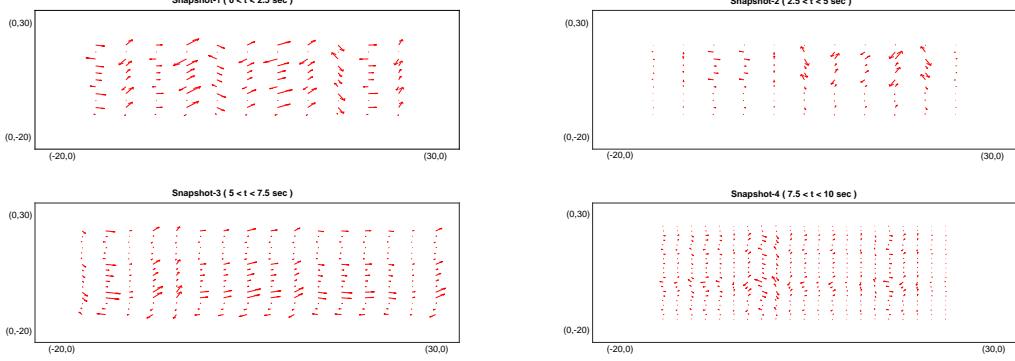


Figure 5.16: Wind turbulence in the domain during localization via consensus

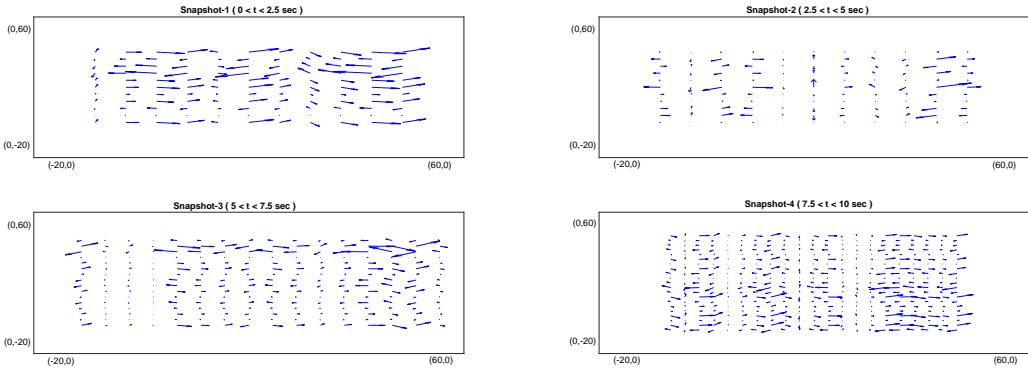
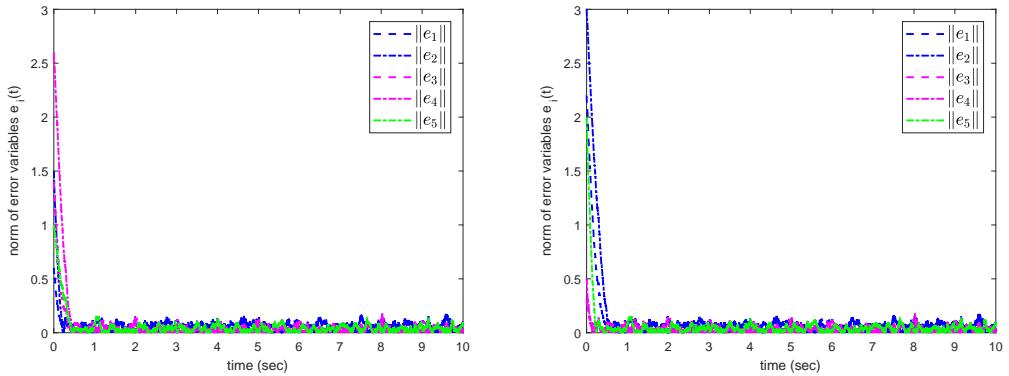


Figure 5.17: Wind turbulence in the domain during localization via formation



(a) Norm of tracking errors along first axis (b) Norm of tracking errors along second axis

Figure 5.18: Norm of tracking errors along both axes in \mathbb{R}^2 (in context of heterogeneous agents)

in figures 5.19 and 5.20 to illustrate the efficacy of the proposed scheme. Figure 5.19 shows the localization under consensus in \mathbb{R}^2 . The domain for this task has been set to be a grid of 50×50 along both the axes. Abscissa ranges from -20

to 30, and so does the ordinate. Start position of agents are denoted by a \times in five different colours. Filaments or the odor molecules are released from the odor source and the molecules disperse in the domain. Figure 5.20 shows agents making parallel formation in \mathbb{R}^2 to locate the source (domain of localization is defined via axis limits, which happens to be a grid of 80×80). In the formation case, abscissa and ordinate range from -20 to 60. The explanation is similar to that for the case of localization via consensus. The performance metrics of the localization in terms of average time spent to locate the source of odor have been provided in table 5.6.

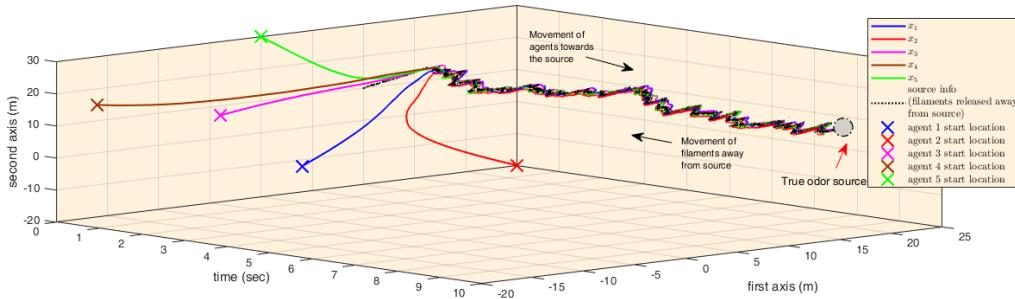


Figure 5.19: Heterogeneous agents in consensus to locate source of odour in \mathbb{R}^2

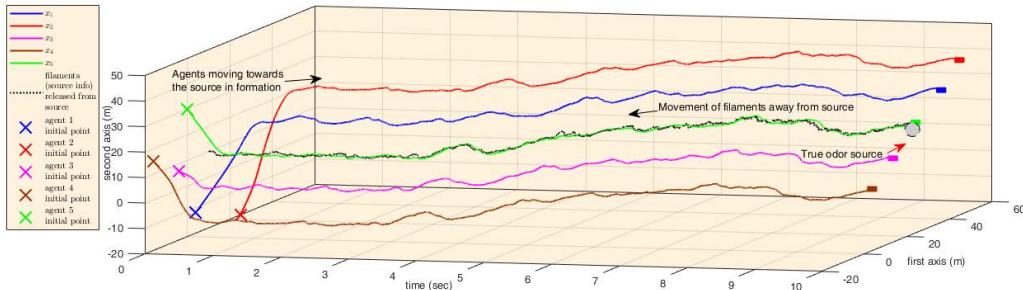


Figure 5.20: Heterogeneous agents in formation to locate source of odour in \mathbb{R}^2

Chapter 6

CONCLUDING REMARKS

An idealist is one who, on noticing that roses smell better than a cabbage, concludes that it will also make better soup.

H. L. Mencken

6.1 Conclusion

This thesis has presented a study on cooperative control of multi-agent systems tasked to locate source of an odor under communication constraints. Contrary to bio-inspired techniques, the proposed algorithm is faster, robust to anomalies, and has a success rate of 100%. Based on the studies so far, there are three main inferences that can be drawn.

1. There exists a global concentration maxima in the immediate vicinity of the true odor source.
2. There exist several local concentration minima along the plume.
3. Odor arrives in packets.

The localization strategy uses a combination of particle swarm optimization; traditional silkworm moth's surging, casting and searching behavior; and a robust control protocol based on event-triggered sliding modes. The controller has been synthesized in a hierarchical fashion of group decision making, path planning of the leader agent, and distributed cooperative control. In designing efficient localization algorithms, effect of wind has also been considered as wind plays an important role in deciding nature of the plume. A number of repeated trials have been conducted to demonstrate the efficacy of the proposed controller. Use of an event-based strategy helps in achieving low computational and communication cost, and at the same time guarantees reliable robustness. Using the proposed control scheme,

6.2 Summary of contributions

The main contributions of this thesis are fourfold.

1. Individual autonomous agents may have some inherent nonlinear dynamics. This work generalizes the dynamics of the agents as an uncertain nonlinear functions. When these functions are zero, the problem reduces to stabilizing integrator dynamics. When the uncertain functions are all alike, resulting dynamics represent a set of homogeneous agents. Individual autonomous agents might have different dynamics for a practical application. Hence, the consideration of heterogeneous agent dynamics is more close to real situations.
2. The finite time robust controller is based on sliding modes with nonlinear sliding hyperplane and novel inverse sine hyperbolic based reaching law. Consequently, the control signal is smooth and reachability to the manifold is fast. This results in faster localization.
3. The synthesized control protocol ensures stability even in the presence of disturbances and parameter variations.
4. The proposed control is an event-driven controller. Hence, all-to-all communication is not necessary. The controller is updated only when local measurement error violates some predefined conditions (designer fixed accuracy adjustment threshold), thereby ensuring lower communication burden to the computing devices.

6.3 Outlook towards future research

We look forward to extend the study for arbitrary order agents, possibly mixed order agents. Moreover, we shall also try to make the localizing algorithm even faster while guaranteeing cent percent success rate. An investigation of effects of unpredictable variables like wind, temperature and humidity shall also be dealt in more detail in our future research. Further, more complex geometrical formations that might ascertain wider area coverage and faster localization shall also be discussed.

BIBLIOGRAPHY

- [1] Renaissence– Illuminating Science & Reason, “Mill of humanity–swarms, emergence and us,” <https://renaissance.com/tag/ants/>, Jul 2017. [Online]. Available: <https://renaissance.com/tag/ants/>
- [2] C. Sarafoleanu, C. Mella, M. Georgescu, and C. Perederco, “The importance of the olfactory sense in the human behavior and evolution,” *J Med Life*, vol. 2, no. 2, pp. 196–198, Apr 2009, jMedLife-02-196[PII]. [Online]. Available: <http://www.ncbi.nlm.nih.gov/pmc/articles/PMC3018978/>
- [3] V. Formisano, S. Atreya, T. Encrenaz, N. Ignatiev, and M. Giuranna, “Detection of methane in the atmosphere of mars,” *Science*, vol. 306, no. 5702, pp. 1758–1761, 2004. [Online]. Available: <http://science.sciencemag.org/content/306/5702/1758>
- [4] V. A. Krasnopolsky, J. P. Maillard, and T. C. Owen, “Detection of methane in the martian atmosphere: evidence for life?” *Icarus*, vol. 172, no. 2, pp. 537 – 547, 2004. [Online]. Available: <http://www.sciencedirect.com/science/article/pii/S0019103504002222>
- [5] F. Lefevre and F. Forget, “Observed variations of methane on mars unexplained by known atmospheric chemistry and physics,” *Nature*, vol. 460, no. 7256, pp. 720–723, Aug 2009. [Online]. Available: <http://dx.doi.org/10.1038/nature08228>
- [6] M. J. Mumma, G. L. Villanueva, R. E. Novak, T. Hewagama, B. P. Bonev, M. A. DiSanti, A. M. Mandell, and M. D. Smith, “Strong release of methane on mars in northern summer 2003,” *Science*, vol. 323, no. 5917, pp. 1041–1045, 2009. [Online]. Available: <http://science.sciencemag.org/content/323/5917/1041>
- [7] K. Zahnle, R. S. Freedman, and D. C. Catling, “Is there methane on mars?” *Icarus*, vol. 212, no. 2, pp. 493 – 503, 2011. [Online]. Available: <http://www.sciencedirect.com/science/article/pii/S001910351000446X>
- [8] Gary Chartrand, Linda Lesniak, Ping Zhang, *Graphs & Digraphs, Sixth Edition*, ser. Textbooks in Mathematics. CRC Press- Taylor and Francis Group, 2015.
- [9] N. Deo, *Graph Theory with Applications to Engineering and Computer Science (Prentice Hall Series in Automatic Computation)*. Upper Saddle River, NJ, USA: Prentice-Hall, Inc., 1974.
- [10] Bollobas Bella, *Modern Graph Theory*. Springer- Verlag, 1998. [Online]. Available: <http://www.springer.com/in/book/9780387984889>

- [11] Fan R. K. Chung, *Spectral Graph Theory*, ser. CBMS Regional Conference Series in Mathematics. AMS and CBMS, 1997, vol. 92. [Online]. Available: <http://bookstore.ams.org/cbms-92>
- [12] Jonathan L. Gross, Jay Yellen, Ping Zhang, *Handbook of Graph Theory, Second Edition*, ser. Discrete Mathematics and Its Applications. CRC Press- Taylor and Francis Group, 2013. [Online]. Available: <http://dx.doi.org/10.1201/b16132>
- [13] K. D. Young, V. I. Utkin, and U. Ozguner, “A control engineer’s guide to sliding mode control,” *IEEE Transactions on Control Systems Technology*, vol. 7, no. 3, pp. 328–342, May 1999.
- [14] Yan, Xing-Gang, Spurgeon, Sarah K., Edwards, Christopher, *Variable Structure Control of Complex Systems*. Springer, 2017.
- [15] Edwards, Christopher, Spurgeon, Sarah K., *Sliding Mode Control: Theory And Applications*. CRC Press- Taylor and Francis Group, 1998.
- [16] A. Sabanovic, Leonid Fridman and S. Spurgeon, Ed., *Variable Structure Systems: from principles to implementation*, ser. Control, Robotics and Sensors. Institution of Engineering and Technology, 2004. [Online]. Available: <http://digital-library.theiet.org/content/books/ce/pbce066e>
- [17] S. H. Zak, *Systems and Control*. 198 Madison Avenue, New York, New York, 10016: Oxford University Press, 2003.
- [18] K. J. Astrom and B. M. Bernhardsson, “Comparison of riemann and lebesgue sampling for first order stochastic systems,” in *Proceedings of the 41st IEEE Conference on Decision and Control, 2002.*, vol. 2, Dec 2002, pp. 2011–2016 vol.2.
- [19] A. Astolfi and L. Marconi, *Analysis and design of nonlinear control systems (in honour of Alberto Isidori)*. Springer- Verlag, 2007.
- [20] A. K. Behera and B. Bandyopadhyay, “Event based robust stabilization of linear systems,” in *IECON 2014 - 40th Annual Conference of the IEEE Industrial Electronics Society*, Oct 2014, pp. 133–138.
- [21] Dawei Shi, Ling Shi and Tongwen Chen, *Event based state estimation- A Stochastic Perspective*. Springer, 2016.
- [22] M. Mazo and P. Tabuada, “Decentralized event-triggered control over wireless sensor/actuator networks,” *IEEE Transactions on Automatic Control*, vol. 56, no. 10, pp. 2456–2461, Oct 2011.
- [23] P. Tabuada, “Event-triggered real-time scheduling of stabilizing control tasks,” *IEEE Transactions on Automatic Control*, vol. 52, no. 9, pp. 1680–1685, Sept 2007.

- [24] K. J. Aström, *Event Based Control*. Berlin, Heidelberg: Springer Berlin Heidelberg, 2008, pp. 127–147.
- [25] A. Anta and P. Tabuada, “To sample or not to sample: Self-triggered control for nonlinear systems,” *IEEE Transactions on Automatic Control*, vol. 55, no. 9, pp. 2030–2042, Sept 2010.
- [26] P. Tallapragada and N. Chopra, “On event triggered tracking for nonlinear systems,” *IEEE Transactions on Automatic Control*, vol. 58, no. 9, pp. 2343–2348, Sept 2013.
- [27] M. Lemmon, *Event-Triggered Feedback in Control, Estimation, and Optimization*. London: Springer London, 2010, pp. 293–358.
- [28] A. Sinha and R. Kumar Mishra, “Temperature regulation in a Continuous Stirred Tank Reactor using event triggered sliding mode control,” in *IFAC Third International Conference on Advances in Control and Optimization Of Dynamical Systems (ACODS 2018)*, Hyderabad, India, Feb. 2018, accepted in IFAC Third International Conference on Advances in Control & Optimization of Dynamical Systems (ACODS-2018). [Online]. Available: <https://hal.archives-ouvertes.fr/hal-01659847>
- [29] A. Sinha and R. K. Mishra, “Control of a nonlinear continuous stirred tank reactor via event triggered sliding modes,” *ArXiv e-prints*, Dec. 2017.
- [30] Sinha, A. and Mishra, R. K., “Consensus tracking in multi agent system with nonlinear and non identical dynamics via event driven sliding modes,” *ArXiv e-prints*, Dec. 2017.
- [31] E. L. Hines, E. Llobet, and J. W. Gardner, “Electronic noses: a review of signal processing techniques,” *IEE Proceedings - Circuits, Devices and Systems*, vol. 146, no. 6, pp. 297–310, Dec 1999. [Online]. Available: <https://doi.org/10.1049/ip-cds:19990670>
- [32] G. Kowadlo and R. A. Russell, “Robot odor localization: A taxonomy and survey,” *The International Journal of Robotics Research*, vol. 27, no. 8, pp. 869–894, 2008. [Online]. Available: <https://doi.org/10.1177/0278364908095118>
- [33] J. G. Monroy, J. González-Jiménez, and J. L. Blanco, “Overcoming the slow recovery of mox gas sensors through a system modeling approach,” *Sensors*, vol. 12, no. 10, pp. 13 664–13 680, 2012. [Online]. Available: <http://www.mdpi.com/1424-8220/12/10/13664>
- [34] G.D.R., “Micrometeorology. by o. g. sutton. new york (mcgraw-hill), 1953. pp. xii, 333; 35 figs., 30 tables. 61s,” *Quarterly Journal of the Royal Meteorological Society*, vol. 79, no. 341, pp. 457–457, 1953. [Online]. Available: <http://dx.doi.org/10.1002/qj.49707934125>

- [35] J. A. Farrell, J. Murlis, X. Long, W. Li, and R. T. Cardé, “Filament-based atmospheric dispersion model to achieve short time-scale structure of odor plumes,” *Environmental Fluid Mechanics*, vol. 2, no. 1, pp. 143–169, Jun 2002. [Online]. Available: <https://doi.org/10.1023/A:1016283702837>
- [36] A. Marjovi and L. Marques, “Optimal spatial formation of swarm robotic gas sensors in odor plume finding,” *Autonomous Robots*, vol. 35, no. 2, pp. 93–109, Oct 2013. [Online]. Available: <https://doi.org/10.1007/s10514-013-9336-1>
- [37] M. H. E. Larcombe, *Robotics in nuclear engineering: Computer assisted teleoperation in hazardous environments with particular reference to radiation fields*. United States: Graham and Trotman, Inc, 1984.
- [38] R. Rozas, J. Morales, and D. Vega, “Artificial smell detection for robotic navigation,” in *Advanced Robotics, 1991. ‘Robots in Unstructured Environments’, 91 ICAR., Fifth International Conference on*, June 1991, pp. 1730–1733 vol.2.
- [39] V. Genovese, P. Dario, R. Magni, and L. Odetti, “Self organizing behavior and swarm intelligence in a pack of mobile miniature robots in search of pollutants,” in *Proceedings of the IEEE/RSJ International Conference on Intelligent Robots and Systems*, vol. 3, Jul 1992, pp. 1575–1582.
- [40] L. Buscemi, M. Prati, and G. Sandini, “Cellular robotics: Behaviour in polluted environments,” in *Proceedings of the 2nd International Symposium on Distributed Autonomous Robotic Systems*, 1994.
- [41] R. Russell, *Chemical source location and the RoboMole project*. Australian Robotics and Automation Association, 2003, pp. 1 – 6.
- [42] R. A. Russell, “Locating underground chemical sources by tracking chemical gradients in 3 dimensions,” in *2004 IEEE/RSJ International Conference on Intelligent Robots and Systems (IROS) (IEEE Cat. No.04CH37566)*, vol. 1, Sept 2004, pp. 325–330 vol.1.
- [43] Russell, R. Andrew, “Robotic location of underground chemical sources,” *Robotica*, vol. 22, no. 1, pp. 109–115, 2004.
- [44] D. Martinez, L. Perrinet, and D. Walther, “Cooperation between vision and olfaction in a koala robot,” in *Report on the 2002 Workshop on Neuromorphic Engineering*, 2002, pp. 51–53.
- [45] A. Loutfi, S. Coradeschi, L. Karlsson, and M. Broxvall, “Putting olfaction into action: using an electronic nose on a multi-sensing mobile robot,” in *2004 IEEE/RSJ International Conference on Intelligent Robots and Systems (IROS) (IEEE Cat. No.04CH37566)*, vol. 1, Sept 2004, pp. 337–342 vol.1.
- [46] H. Ishida, K. Yoshikawa, and T. Moriizumi, “Three-dimensional gas-plume tracking using gas sensors and ultrasonic anemometer,” in *Proceedings of IEEE Sensors, 2004.*, Oct 2004, pp. 1175–1178 vol.3.

- [47] H. Ishida, A. Kobayashi, T. Nakamoto, and T. Moriizumi, “Three-dimensional odor compass,” *IEEE Transactions on Robotics and Automation*, vol. 15, no. 2, pp. 251–257, Apr 1999.
- [48] T. Nakamoto, H. Ishida, and T. Moriizumi, “An odor compass for localizing an odor source,” *Sensors and Actuators B: Chemical*, vol. 35, no. 1, pp. 32 – 36, 1996, proceedings of the Sixth International Meeting on Chemical Sensors. [Online]. Available: <http://www.sciencedirect.com/science/article/pii/S0925400596020096>
- [49] H. Ishida, T. Nakamoto, and T. Moriizumi, “Study of odor compass,” in *1996 IEEE/SICE/RSJ International Conference on Multisensor Fusion and Integration for Intelligent Systems (Cat. No.96TH8242)*, Dec 1996, pp. 222–226.
- [50] H. Matsukura, H. Hashiguchi, and H. Ishida, “Olfactory search behavior of human wearing olfactory assist mask,” in *IEEE SENSORS 2014 Proceedings*, Nov 2014, pp. 1976–1979.
- [51] R. Russell, A. Bab-Hadiashar, R. L. Shepherd, and G. G. Wallace, “A comparison of reactive robot chemotaxis algorithms,” *Robotics and Autonomous Systems*, vol. 45, no. 2, pp. 83 – 97, 2003. [Online]. Available: <http://www.sciencedirect.com/science/article/pii/S0921889003001209>
- [52] J. A. Farrell, S. Pang, and W. Li, “Plume mapping via hidden markov methods,” *IEEE Transactions on Systems, Man, and Cybernetics, Part B (Cybernetics)*, vol. 33, no. 6, pp. 850–863, Dec 2003.
- [53] S. Pang and J. A. Farrell, “Chemical plume source localization,” *IEEE Transactions on Systems, Man, and Cybernetics, Part B (Cybernetics)*, vol. 36, no. 5, pp. 1068–1080, Oct 2006.
- [54] M. Vergassola, E. Villermaux, and B. Shraiman, ““Infotaxis” as a strategy for searching without gradients,” *Nature*, vol. 445, no. 7126, pp. 406–409, 2007. [Online]. Available: <https://hal.archives-ouvertes.fr/hal-00326807>
- [55] D. Zarzhitsky, “Physics-based approach to chemical source localization using mobile robotic swarms,” Ph.D. dissertation, University of Wyoming, Laramie, WY, USA, 2008, aAI3338814.
- [56] D. Zarzhitsky and D. F. Spears, “Swarm approach to chemical source localization,” in *2005 IEEE International Conference on Systems, Man and Cybernetics*, vol. 2, Oct 2005, pp. 1435–1440.
- [57] V. Braitenberg, *Vehicles: Experiments in Synthetic Psychology*. Boston, MA, USA: MIT Press, 1984.

- [58] C. Lytridis, G. S. Virk, Y. Rebour, and E. E. Kadar, “Odor-based navigational strategies for mobile agents,” *Adapt. Behav.*, vol. 9, no. 3-4, pp. 171–187, Apr. 2001. [Online]. Available: <http://dx.doi.org/10.1177/10597123010093004>
- [59] H. Ishida, K. Suetsugu, T. Nakamoto, and T. Moriizumi, “Study of autonomous mobile sensing system for localization of odor source using gas sensors and anemometric sensors,” *Sensors and Actuators A: Physical*, vol. 45, no. 2, pp. 153 – 157, 1994. [Online]. Available: <http://www.sciencedirect.com/science/article/pii/0924424794008299>
- [60] L. Marques and A. T. D. Almeida, “Electronic nose-based odour source localization,” in *6th International Workshop on Advanced Motion Control. Proceedings (Cat. No.00TH8494)*, April 2000, pp. 36–40.
- [61] L. Marques, U. Nunes, and A. T. de Almeida, “Olfaction-based mobile robot navigation,” *Thin Solid Films*, vol. 418, no. 1, pp. 51 – 58, 2002, proceedings from the International School on Gas Sensors in conjunction with the 3rd European School of the NOSE Network. [Online]. Available: <http://www.sciencedirect.com/science/article/pii/S004060900200593X>
- [62] C. W. Reynolds, “Flocks, herds and schools: A distributed behavioral model,” *SIGGRAPH Comput. Graph.*, vol. 21, no. 4, pp. 25–34, Aug. 1987. [Online]. Available: <http://doi.acm.org/10.1145/37402.37406>
- [63] W. Ren and R. W. Beard, “Consensus seeking in multiagent systems under dynamically changing interaction topologies,” *IEEE Transactions on Automatic Control*, vol. 50, no. 5, pp. 655–661, May 2005.
- [64] R. Olfati-Saber, J. A. Fax, and R. M. Murray, “Consensus and cooperation in networked multi-agent systems,” *Proceedings of the IEEE*, vol. 95, no. 1, pp. 215–233, Jan 2007.
- [65] W. Yu, G. Chen, W. Ren, J. Kurths, and W. X. Zheng, “Distributed higher order consensus protocols in multiagent dynamical systems,” *IEEE Transactions on Circuits and Systems I: Regular Papers*, vol. 58, no. 8, pp. 1924–1932, Aug 2011.
- [66] Hayes, Adam T. and Martinoli, Alcherio and Goodman, Rodney M., “Swarm robotic odor localization: Off-line optimization and validation with real robots,” *Robotica*, vol. 21, no. 4, pp. 427–441, Aug. 2003. [Online]. Available: <http://dx.doi.org/10.1017/S0263574703004946>
- [67] J. Kennedy and R. Eberhart, “Particle swarm optimization,” in *Neural Networks, 1995. Proceedings., IEEE International Conference on*, vol. 4, Nov 1995, pp. 1942–1948 vol.4.
- [68] L. Marques, U. Nunes, and A. T. de Almeida, “Particle swarm-based olfactory guided search,” *Autonomous Robots*, vol. 20, no. 3, pp. 277–287, Jun 2006. [Online]. Available: <https://doi.org/10.1007/s10514-006-7567-0>

- [69] W. Jatmiko, K. Sekiyama, and T. Fukuda, “A pso-based mobile robot for odor source localization in dynamic advection-diffusion with obstacles environment: theory, simulation and measurement,” *IEEE Computational Intelligence Magazine*, vol. 2, no. 2, pp. 37–51, May 2007.
- [70] Q. Lu, S. r. Liu, and X. n. Qiu, “A distributed architecture with two layers for odor source localization in multi-robot systems,” in *IEEE Congress on Evolutionary Computation*, July 2010, pp. 1–7.
- [71] Q. Lu and Q. L. Han, “Decision-making in a multi-robot system for odor source localization,” in *IECON 2011 - 37th Annual Conference of the IEEE Industrial Electronics Society*, Nov 2011, pp. 74–79.
- [72] Q. Lu and Q.-L. Han, “A probability particle swarm optimizer with information-sharing mechanism for odor source localization,” *IFAC Proceedings Volumes*, vol. 44, no. 1, pp. 9440 – 9445, 2011, 18th IFAC World Congress. [Online]. Available: <http://www.sciencedirect.com/science/article/pii/S1474667016451281>
- [73] Q. Lu, Q. L. Han, X. Xie, and S. Liu, “A finite-time motion control strategy for odor source localization,” *IEEE Transactions on Industrial Electronics*, vol. 61, no. 10, pp. 5419–5430, Oct 2014.
- [74] E. D. Sontag, *Input to State Stability: Basic Concepts and Results*. Berlin, Heidelberg: Springer Berlin Heidelberg, 2008, pp. 163–220. [Online]. Available: https://doi.org/10.1007/978-3-540-77653-6_3
- [75] Hasan K. Khalil, *Nonlinear Systems, Third Edition*. Upper Saddle River, NJ, USA: Prentice-Hall, Inc., 2002.
- [76] Alexander G. Ramm, Nguyen S. Hoang, *Dynamical Systems Method and Applications: Theoretical Developments and Numerical Examples*. Wiley, 2011.
- [77] A. Sinha, R. Kaur, R. Kumar, and A. P. Bhondekar, “Cooperative control of multi-agent systems to locate source of an odor,” *ArXiv e-prints*, Nov. 2017.
- [78] M. L. Cao, Q. H. Meng, Y. X. Wu, M. Zeng, and W. Li, “Consensus based distributed concentration-weighted summation algorithm for gas-leakage source localization using a wireless sensor network,” in *Proceedings of the 32nd Chinese Control Conference*, July 2013, pp. 7398–7403.
- [79] J. Matthes, L. Groll, and H. B. Keller, “Source localization by spatially distributed electronic noses for advection and diffusion,” *IEEE Transactions on Signal Processing*, vol. 53, no. 5, pp. 1711–1719, May 2005.

INDEX

A			
above-ground agents		autonomy	39
14		avalanches	4
abscissa	35, 41	average time	42
acceleration		axis limits	41, 45
coefficients	20		
accumulated average			
22			
accuracy adjustment			
19			
accuracy parameter	32		
accuracy threshold	19		
accurate	36	bacteria	3
actual	33	balanced	8
actuation	15	bandwidth	9, 26
actuator constraints		bio-inspired	
23, 33		algorithms	14
adjacency matrix	7	biological systems	6
adjacent	33	blue crabs	3
admissible	30	bounded	34
advection	32	bounds	30
agent maneuvering	14	Braitenberg style	14
airflow velocity	32	burden	9
ambiguity	24	butane	4
amplitude statistics	13		
anemometers	32	C	
anemotaxis	2, 14	capabilities	10
anomalies	46	casting	19, 22
ants	3	central processing unit	
architectures	26	10	
ascending	28	chattering	24
asymptotically		chattering free	41
cooperatively		chemical gradient	14
stable	7	chemically sensitive	
attractive	9, 23, 27	robots	14
audition	1	chemotactic	2
		chemotaxis	2, 14
		chronoception	1
		circuits	26
		clock pulse	28
		closed loop activity	5
		closed loop performance	
		10	
		collaborative manner	6
		collective entity	6
		common goal	6
		communication	9
		communication	
		channel	26
		communication	
		constraints	
		17, 19, 46	
		communication link	17
		communication links	7
		communication	
		resources	26
		Comparison Lemma	30
		Complex systems	6
		comprising	28
		computational	9, 26
		computational	
		expense	11
		computational	
		requirements	
		34	
		computational unit	26
		concentration gradient	
		14	
		consecutive agents	39
		consensus	7, 25, 33, 39
		constrained	26, 27
		control effort	23
		control framework	17
		control implementation	
		34	
		control of the robot	6

control protocol	26, 27	discontinuous control	energy	9	
controller updates	34, 40	discontinuous control effort	energy constrained environments	16	
convergence	7, 33, 39, 42	discretization	energy expenditure	15	
convergence time	25	discretization error	energy expenses	10, 34	
cooperation	6	29	entities	6	
cooperative control	6, 15	disperse	equilibrioception	1	
cooperative controllability	7	dispersion model	equilibrium point	6, 32	
cooperatively stable	7	distributed cooperative algorithm	equipped sensors	33	
coordinates	33	distributed	equivalent control	9	
correlated	32	coordination	Escherichia coli	3	
cost	17	control	estimated	32	
customs	4	distributed sensing	estimation	32	
D					
decrease	27	domain	Euler's constant	25	
degree matrix	7	dominance	event	9, 26	
derivative	28	downwind	event based control	10	
design parameters	32, 33	drugs	Event based sampling	26	
desired convergence	33, 40	dynamic	event triggering	9	
diagonal matrix	7	dynamic plume	event-based	34	
differential inequality	30	dynamical models	event-based control	26	
differentially driven	15	dynamical optimization	event-based control scheduling	19	
diffusing material	33	E			
diffusion	32	E. coli algorithm	Event-based sampling	10, 26	
diffusion dominated	32	earthquake	event-based sliding modes	19	
diffusion-advection	32	echolocation	event-based strategies	10	
digraph	7, 31	edge	event-driven design	26	
directed edge	8	efficiency	event-triggered	42	
directed path	7	eigenvalue	execution	29	
directed topology	18, 25	eigenvalues	exigent need	26	
		electrical charge	existence	27	
		theory	exogenous	17	
		electronic nose	expensive	26	
		electroreception	experiment	32	
		elimination			
		embedded systems			

exploration	22	governing dynamics	18	inertia factor	20
exploratory behavior	15	graph matrices	31	information sharing	
exponential	28	graph theory	7	matrix	16
F		grid	44	infotaxis	14
familiarity	1	group consensus	34	inherent non-linearity	
faster convergence	17	group phenomena	6	18	
feedback law	18	H		inherent robustness	8
fewer samples	34	hearing	1	Initial conditions	32
filament release rate	33	heat losses	34	initial position	33
filaments	39	heterogeneity	16	input-to-state stable	18
finite time	33, 39	heterogeneous agents		instability	23
fire	4	39		instantaneous gradient	
first axis	35, 41	heterogeneous		dependency	
fish	3	multi-agent		14	
fixed distance	39	systems	18	instantaneous plume	
fixed sampling rate	10	hierarchical		sensing	6, 18
fluctuations	9, 28	cooperative		integrator dynamics	15
fluxotaxis	14	control	17	integrator systems	18
followers	18	higher dimensions	18	intelligent control	
forcing function	24	hill	4	protocols	17
forest	4	homogeneous	15	intelligent mechanism	
formation	33, 42	homogeneous agents		of perception	
forward approach	2	18, 33		of odor	5
fresh value	28	human activity	4	inter-event execution	
full rank	8	humanitarian	2	time	30
G		humidity	13	interaction	31
gain	23	hybrid	11	interconnected	17
gain tuning	24	hygroreception	1	interoception	1
gas leaks	4	hypergeometric		inverse approach	2
gas sensors	32	manifold	8	inverse hyperbolic	24
Gaussian distribution		hyperplane	8	invertible	25
14		I		K	
Gaussian plume	13	incidence matrix	8	kitchen	4
geometrical pattern	42	indispensable	26	Kronecker products	18
global best	15	industrial setups	4	L	
globally attractive	28	inequality	30	landslides	4
				Laplacian	7

large scale interconnected systems	matched perturbations	movement trajectory
large-scale latency	maximum likelihood estimation	multi-agent swarm
leader	mean	multi-agent systems
leader agent	mean airflow	multiple mobile agents
least squares	mean airflow velocity	
Lebesgue sampling	21	
limited bandwidth	mean odor concentration	
limited communication	meandering	N
line of communication	measure of error	necessary
linear sliding manifolds	mechanical systems	negative definite
Lipschitz	mechatronic	neighbors
lobsters	median localization	networked control
local best	time	networked systems
local information	metal oxide gas sensors	nociception
local maximum	meteorological condition	nodes
local measurement error	microcontrollers	noise
localization	Microorganisms	nominal system
localization problem	minima	non singularity
long term time average	minimal	non-holonomic
lower bound	mismatched	non-identical
Lyapunov function	mismatched perturbations	non-trivial odor
Lyapunov function candidate	42	non-uniform sampling
M	mobile platform	nonlinear gain
magnetoreception	molecular diffusion	nonlinear sliding
manifestations	monotonous	manifold
manifold	mosquitoes	nonlinear sliding
Mars	moths	manifolds
matched	movement of odor	norm
	filaments	noticeable change
	movement process	nuclear industry
	21	nullification
		nullified
		nutrients
		O
		obstacle avoidance
		15

occupancy	10	Particle Swarm Optimization	R
occupying	26		random motion 13
odd	24	15, 19	random process 21
odor compass	14	patchy 12	randomly 39
odor concentration		perception 1	range space 34
patches	12	performance metrics	rapid information exchange 26
odor concentrations	12	37, 43	
odor dispersal	12	periodic sampling 10,	reachability 23
odor filaments	12, 33	26	reachability constant
odor localization	6	periodic update 9, 19	9, 27
Odor molecules	32	perturbations 15	reaching law 24
odor molecules	12, 39	pheromone trails 3	reaching phase 8
odorant	1	physiological	reactive plume
offset	23	potencies 1	tracking 14
oil spills	4	plume emission 13	reactive sensory
olfaction	1	plume model 32	surface 12
olfactory assisted		plume tracking 39	realistic 32
mask	14	positive quantities 30	recollection 1
olfactory environment		power consumption 26	redundancy 15
13		predefined threshold	reference 23
olfactory potencies	12	10	reference state 34
operational efficiency		predicted 33, 39	reference tracking 25
15		predicted location 18	releasing time 22
operational lifetime	34	probability density	repeated trials 34
opinion	23	function 14	resource utilization 26
ordinate	35, 41	probability of success	resources 9, 26
originate	33	15	response time 13
oscillation center	19	probability PSO 16	Reynold's number 12
overall economy	17	processor time 26	Riemann sampling 10
		proportional-only	robot maneuvering 6
		controller 15,	Robot olfaction 4
		20	robot olfaction 6
P			
packet loss	7	proposition 34	robust 17
packets	46	proprioception 1	robust controller 19
parallel	33	pseudo-Gaussian	robustness 34, 39
parallel formation	34,	plume 14	root 8
	39, 42		
parasitoid wasps	3	Q	S
particle filter	15	quarantine 4	sacrificing 34

sample instants	10	source	33	system performance
sampled data	9	source information	39	23
samples	26	spanning tree	8	system trajectories 27
Sampling	26	spatial diversity	15	systems 26
sampling	10	speed of convergence		
sampling frequency	10		23	T
sampling instant	29	spread out	36	tailoring 33
sampling intervals	34	stability	28	taste 1
saturates	34	stability problem	7	tear 34
search and rescue	4	stabilizing	25	telemetry 17
searching	19, 22	standard deviation	22	temperature 13
second axis	35, 41	state evolution	26	temporal statistics 14
semantic information	5	state space	8, 23	thermal effects 32
sensitivity	13	state velocity vectors	9	thermoception 1
sensor data fusion	5	static electronic noses		time shared 26
separation	33		12	time varying 32
shared network	26	stationary	13	time-based 34
sight	1	statistics	34	time-triggered 42
silkworm moth style	14	steady concentration		tolerate 28
simulations	31		32	touch 1
single filament	21	steady state	26	tracking controller 19,
sliding	9	sub-optimal	26	33
sliding manifold	8	sub-system	6	tracking error 39
sliding mode	23, 27	success rate	17, 34, 42	tracking errors 33
sliding mode control	8	successive sampling		tracking reference 20
sliding motion	23	instants	28	trade-off 10
sliding phase	9	sufficient	27	traditional sliding
sliding regime	23, 34	surface	8, 23	mode 34
slope	23	surging	19, 22	trail 4
smell	1	swarm intelligence	15	transmission 10
smooth	24, 34	switching	8	transmitting 26
smooth control	40	switching circuitry	34	triangulation 16
snapshots	43	switching topology	31	triggering 26
sniffing animals	2	Synchronous	26	triggering rule 28
sniffing robots	4	synergistic integration		triggers 30
social systems	6		5	tuning 40
solution	30	synthesize	17	turbulence 12, 32
somatosensation	1	synthesized	34	turbulence diffusion 32

turbulence diffusion	cooperatively	volatile	2
coefficient 32	stable 7		
turbulence dominated	uniformly sampled 19		W
flow 14	upper bounded 26	waste	26
turbulent diffusion 13		wear	34
turbulent environment	V	wind	32
42	variable structure	wind direction	14
	control 8	wind information	15
	velocity plot 43	wind velocity	32
	vertex 7		
U	vertical axis 10, 33	Z	
uncertain function 18	vertices 7	zero order hold	
uncertainty 17	vicinity 27	operator 10	
underground search 14	violated 28	Zigzag dung beetle	
unexploded mines 4	virtual leader 18, 23, 31	approach 14	
uniformly	vision 1		
asymptotically			